

Supporting Information for:

Curved Polycyclic Aromatic Molecules That Are π -Isoelectronic to Hexabenzocoronene

Jiye Luo,¹ Xiaomin Xu,¹ Renxin Mao,¹ Qian Miao*^{1, 2}

¹*Department of Chemistry, the Chinese University of Hong Kong, Shatin, New Territories, Hong Kong, China*

²*Institute of Molecular Functional Materials (Areas of Excellence Scheme, University Grants Committee), Hong Kong, China*

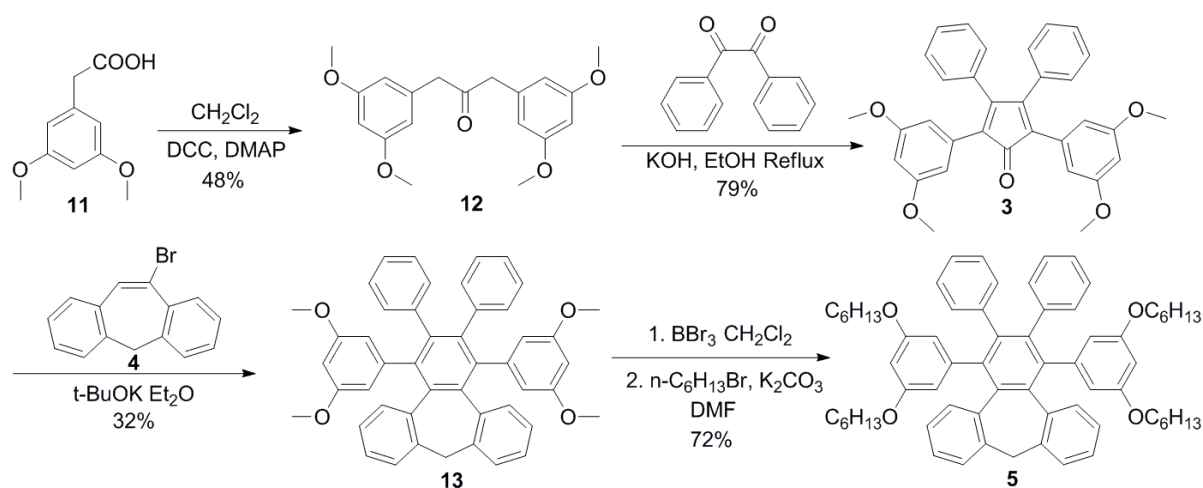
Table of Contents

1. Synthesis
2. Variable temperature ¹H NMR for compounds **1** and **8**.
3. Thermal isomerization of twisted-**2b** and *anti*-**2b**
4. UV-vis absorption spectra
5. DFT calculation
6. Cyclic Voltammetry
7. Fabrication and characterization of solution-deposited thin films and transistors
8. NMR spectra
9. Calculation of Gauss curvature

1. Synthesis

General: The reagents and starting materials employed were commercially available and used without any further purification or made following reported methods. Anhydrous and O₂-free diethyl ether and THF were purified by an Advanced Technology Pure-Solv PS-MD-4 system. NMR spectra were recorded on a Bruker ADVANCE III 400MHz spectrometer (¹H NMR: 400 MHz, ¹³C NMR: 100 MHz). Chemical shift values (δ) are expressed in parts per million using residual solvent protons (¹H NMR, δ_H = 7.26 for CDCl₃, δ_H = 2.50 for DMSO-d₆ and δ_H = 5.32 for CD₂Cl₂; ¹³C NMR, δ_C = 77.16 for CDCl₃, δ_C = 53.84 for CD₂Cl₂) as internal standard. Mass spectra were recorded on a Thermo Finnigan MAT 95 XL spectrometer. X-ray crystallography data were collected on a Bruker AXS Kappa ApexII Duo Diffractometer. UV-vis absorption spectra were recorded on a Varian CARY 1E UV-vis spectrophotometer. Melting points, without correction, were measured using a Nikon Polarized Light Microscope ECLIPSE 50i POL equipped with an INTEC HCS302 heating stage.

Scheme S1 Synthesis of precursor **5**.



1,3-Bis(3,5-dimethoxyphenyl)-2-propanone (**12**)

To a solution of the N, N'-dicyclohexylcarbodiimide (29 g, 0.14 mol) and 4-dimethylaminopyridine (3.9 g, 32 mmol) in 100 ml anhydrous CH₂Cl₂ was added a solution of the 3,5-dimethoxyphenylacetic acid (**11**) (25 g, 0.13 mol, in 50 ml anhydrous CH₂Cl₂). The solution was kept stirred under N₂ at room temperature for 24 hours. Then the resulting yellow suspension was filtered and the filtrate was concentrated under reduced pressure. The crude product was purified by column chromatography on silica gel with ethyl acetate/hexane 1/2 (V/V) as eluent. 1,3-Bis(3,5-dimethoxyphenyl)-2-propanone (**12**) was collected as white solid (10.1 g, 48%). mp: 119-120 °C. ¹H NMR (CDCl₃) δ (ppm): 6.36 (d, *J* = 2.0 Hz, 2H), 6.30 (d, *J* = 2.0 Hz, 4H), 3.76 (s, 12H), 3.64 (s, 4H). ¹³C NMR (CDCl₃) δ (ppm): 205.5, 161.1, 136.2, 107.7, 99.3, 55.4, 49.4. HRMS (EI⁺): calcd. for C₁₉H₂₂O₅ ([M]⁺): 330.1462, found: 330.1468.

2,5-bis(3,5-dimethoxyphenyl)-3,4-diphenylcyclopentadienone (**3**)

To a solution of 1,3-bis(3,5-dimethoxyphenyl)-2-propanone (**12**) (3.30 g, 10 mmol) and benzil (2.31g, 11 mmol) in 50 ml hot EtOH was added a solution of KOH (560 mg, 10 mmol) in 5 ml of ethanol dropwisely. The yellow solution changed to red immediately and then precipitates formed gradually. The suspension was kept stirred for 30 minutes at reflux. Then

the resulting mixture was cooled to 0 °C and filtered. 3.99 g of tetraphenylcyclopentadienone (**3**) was collected as brown solid in a yield of 79%. mp: 202-203 °C. ¹H NMR (CDCl₃) δ (ppm): 7.17-7.24 (m, 6H), 6.95-6.97 (m, 4H), 6.40 (d, *J* = 2.4 Hz, 4H), 6.34 (t, *J* = 2.4 Hz, 2H), 3.59 (s, 12H). ¹³C NMR (CDCl₃) δ (ppm): 200.0, 160.4, 155.0, 133.3, 132.5, 129.4, 128.7, 128.2, 125.3, 108.0, 101.0, 55.3. HRMS (EI⁺): calcd. for C₃₃H₂₈O₅ ([M]⁺): 504.1931, found: 504.1938.

1,4-Bis(3,5-dimethoxyphenyl)-2,3-diphenyl-9H-tribenzo[a,c,e]cycloheptene (13**)**

To a suspension of 2,5-bis(3,5-dimethoxyphenyl)-3,4-diphenylcyclopentadienone (**3**) (1.01 g, 2 mmol) and t-BuOK (448 mg, 4 mmol) in 100 ml of anhydrous diethyl ether was added 1.08 g (4 mmol) of 10-bromo-5H-dibenzo[a,d]cycloheptene (**4**)¹. The resulting mixture was stirred under a nitrogen atmosphere for 24 hours. The reaction was quenched with an aqueous solution of NH₄Cl and the resulting mixture was filtered. The filter cake was washed with H₂O, ethanol and Et₂O subsequently. 427 mg of **13** was obtained as white powder in a yield of 32%. mp: sublimation before melting. ¹H NMR (CDCl₃) δ (ppm): 7.43 (d, *J* = 7.6 Hz, 2H), 7.17 (d, *J* = 7.6 Hz, 2H), 7.04 (t, *J* = 7.6 Hz, 2H), 6.92- 6.97 (m, 4H), 6.83 (t, *J* = 7.6 Hz, 2H), 6.73 (t, *J* = 7.6 Hz, 2H), 6.65 (t, *J* = 7.6 Hz, 2H), 6.51 (d, *J* = 7.6 Hz, 2H), 6.35 (s, 2H), 5.99 (t, *J* = 4.0 Hz, 2H), 5.74 (s, 2H), 4.15 (d, *J* = 12.0 Hz, 1H), 3.64 (d, *J* = 12.0 Hz, 1H), 3.53 (s, 6H), 3.39 (s, 6H). Due to low solubility in common solvents, ¹³C NMR spectrum of molecule **13** was not recorded. HRMS (EI⁺): calcd. for C₄₇H₃₈O₄ ([M]⁺): 666.2765, found: 666.2766.

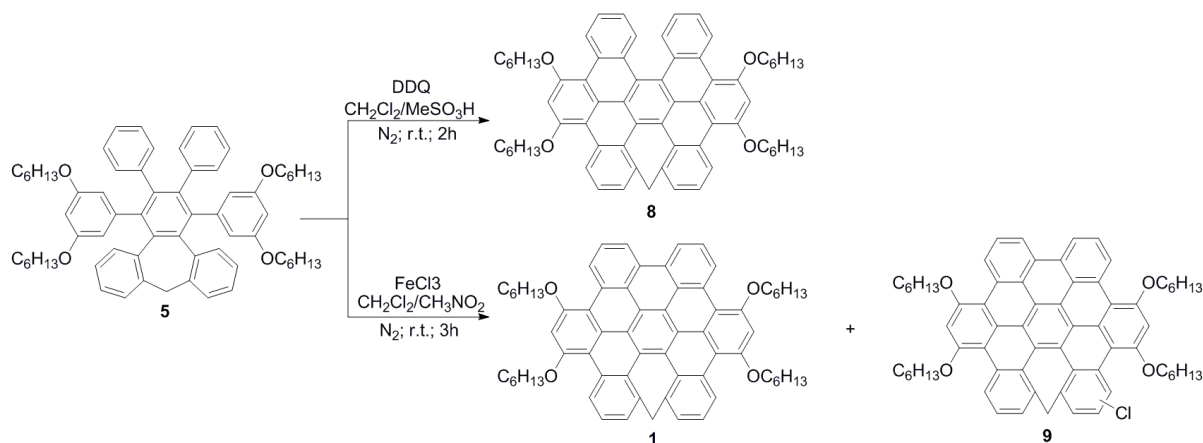
1,4-bis(3,5-dihydroxyphenyl)-2,3-diphenyl-9H-tribenzo[a,c,e]cycloheptene (5**)**

To a solution of **13** (333 mg, 0.5 mmol) in 40 ml of anhydrous CH₂Cl₂ was added a solution of BBr₃ (10 ml, 1M in CH₂Cl₂) at 0 °C under an atmosphere of nitrogen. The solution was warmed to room temperature and heated to reflux for 4 hours. Then the reaction mixture was cooled with ice bath and quenched with H₂O. The mixture was extracted with diethyl ether, washed with water and brine, dried with anhydrous Na₂SO₄, and concentrated under reduced pressure. The crude product of 1,4-bis(3,5-dihydroxyphenyl)-2,3-diphenyl-9H-tribenzo[a,c,e]cycloheptene was collected as light yellow powder and used in the next step without further purification.

To a suspension of crude 1,4-bis(3,5-dihydroxyphenyl)-2,3-diphenyl-9H-tribenzo[a,c,e]cycloheptene and K₂CO₃ (1.38 g, 10 mmol) in 5 ml of DMF was added 1.4 ml of bromohexane (1.65 g, 10 mmol). The solution was heated to 85 °C overnight. Then the reaction was quenched with water, extracted with diethyl ether, washed with water and brine, dried with anhydrous Na₂SO₄. The resulting solution was concentrated under reduced pressure and the crude product was purified by column chromatography on silica gel with CH₂Cl₂/hexane 1/2 (V/V) as eluent. 342 mg (72%) of **5** was obtained as white powder. mp: 121-122 °C. ¹H NMR (CDCl₃) δ (ppm): 7.40 (d, *J* = 7.6 Hz, 2H), 7.15 (d, *J* = 7.6 Hz, 2H), 7.01 (t, *J* = 7.6 Hz, 2H), 6.92- 6.96 (m, 4H), 6.81 (t, *J* = 7.6 Hz, 2H), 6.72 (t, *J* = 7.6 Hz, 2H), 6.65 (t, *J* = 7.6 Hz, 2H), 6.51 (d, *J* = 7.6 Hz, 2H), 6.33 (s, 2H), 5.99 (t, *J* = 2.0 Hz, 2H), 5.71 (s, 2H), 4.13 (d, *J* = 12.0 Hz, 1H), 3.37-3.76 (m, 9H), 1.57-1.62 (dd, *J*₁ = 14.0 Hz, *J*₂ = 6.8 Hz, 4H), 1.46-1.51 (dd, *J*₁ = 14.0 Hz, *J*₂ = 6.8 Hz, 4H), 1.27-1.34 (m, 24H), 0.89-0.93 (m, 12H). ¹³C NMR (CDCl₃) δ (ppm): 158.9, 158.8, 144.7, 142.6, 141.3, 140.8, 140.3, 137.8, 135.9, 132.5, 132.2, 130.3, 127.2, 126.9, 126.0, 125.6, 125.0, 124.8, 112.4, 110.6, 100.7, 68.3, 68.2, 40.8, 31.7, 31.6, 29.2, 29.0, 25.8, 25.7, 22.8, 14.2. HRMS (EI⁺): calcd. for C₆₇H₇₈O₄ ([M]⁺): 947.5973, found: 947.5987.

1. Phillips, S. T.; Depaulis, T.; Neergaard, J. R.; Baron, B. M.; Siegel, B. W.; Seeman, P.; Vantol, H. H. M.; Guan, H. C.; Smith, H. E. *J. Med. Chem.* **1995**, *38*, 708

Scheme S2 Oxidative cyclization reactions of precursor **5**.



Incompletely cyclized product (**8**)

To a solution of **5** (47 mg, 0.05 mmol) in 18 ml of anhydrous CH_2Cl_2 cooled at 0°C was added 2 ml of MeSO_3H and 113 mg of DDQ (0.5 mmol). The colourless solution of reaction mixture turned to black gradually. The reaction was stirred at 0°C under N_2 atmosphere for 2 hours and then was quenched with an aqueous solution of NaHCO_3 and extracted with CH_2Cl_2 . The organic layer was separated and washed with H_2O and brine, dried with anhydrous Na_2SO_4 , then concentrated under reduced pressure. The crude yellow powder was further purified by column chromatography on silica gel with $\text{CH}_2\text{Cl}_2/\text{hexane}$ 1/2(V/V) as eluent. 32 mg of **8** was obtained as yellow powder in a yield of 67%. mp: $196\text{--}197^\circ\text{C}$. ^1H NMR (CDCl_3) δ (ppm): 9.34 (d, $J = 8.0$ Hz, 2H), 9.26 (d, $J = 8.0$ Hz, 2H), 8.20 (d, $J = 8.0$ Hz, 2H), 7.61 (t, $J = 7.6$ Hz, 2H), 7.54 (d, $J = 6.4$ Hz, 2H), 7.40 (t, $J = 7.6$ Hz, 2H), 7.19 (s, 2H), 7.12 (t, $J = 7.6$ Hz, 2H), 4.38 (br, 4H), 4.24 (br, 4H), 4.10 (br, 1H), 3.83 (br, 1H), 2.08–2.15 (m, 4H), 1.94–1.99 (m, 4H), 1.69–1.72 (m, 4H), 1.57–1.60 (m, 4H), 1.36–1.50 (m, 16H), 0.96 (t, $J = 7.2$ Hz, 6H), 0.90 (t, $J = 7.2$ Hz, 6H). ^{13}C NMR (CDCl_3) δ (ppm): 156.22, 156.19, 139.5, 131.1, 130.7, 129.2, 129.1, 128.2, 127.5, 127.1, 126.7, 126.3, 125.9, 124.6, 123.9, 123.6, 123.4, 112.8, 111.9, 100.1, 70.4, 69.9, 43.7, 31.8, 31.7, 29.7, 29.6, 26.3, 26.1, 22.8, 22.7, 14.2, 14.1. HRMS (EI^+): calcd. for $\text{C}_{67}\text{H}_{70}\text{O}_4$ ($[\text{M}]^+$): 938.5269, found: 938.5280.

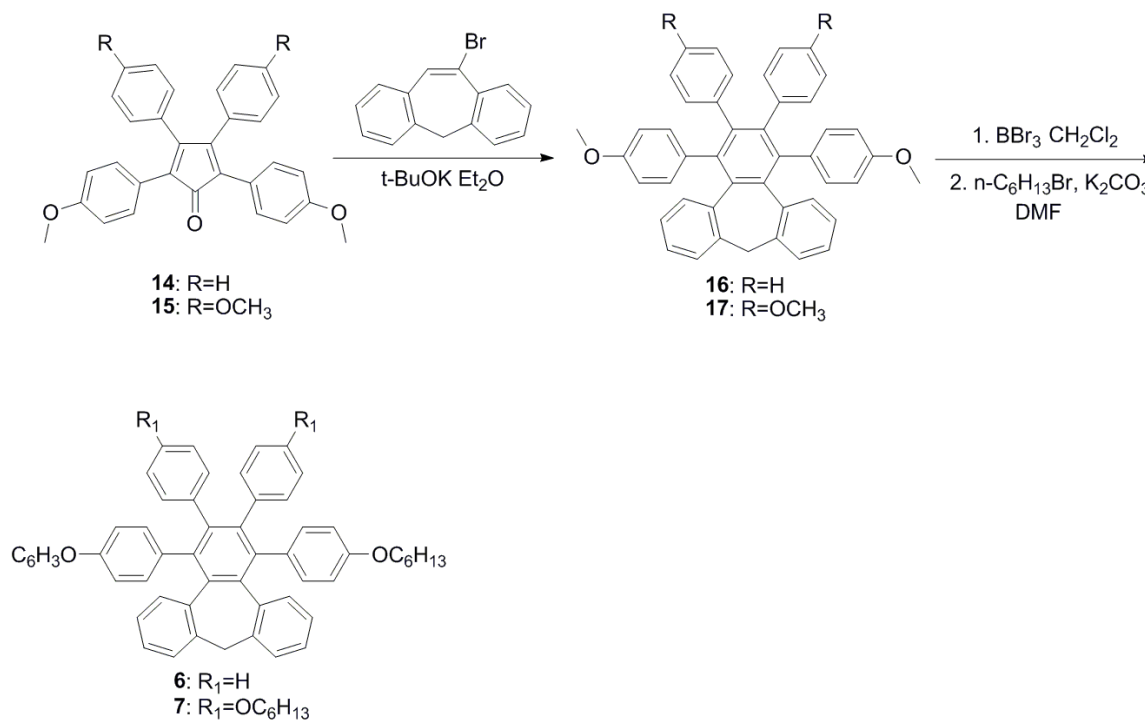
Heptagon-embedded HBC **1**

A solution of **5** (47 mg, 0.05 mmol) in 50 ml of anhydrous CH_2Cl_2 was bubbled with N_2 for 10 minutes, and then was added 245 mg (1.5 mmol, 30 eq) of FeCl_3 in 1 ml CH_3NO_2 . The reaction mixture turned to a black solution immediately, which was stirred with a flow of nitrogen bubbling through for 3 hours. The resulting solution was quenched with methanol followed with H_2O . The resulting mixture was extracted with CH_2Cl_2 . The organic phase was washed with H_2O and brine, dried with anhydrous Na_2SO_4 , then concentrated under reduced pressure. The yellow powder of crude product was further purified by column chromatography on silica gel with $\text{CH}_2\text{Cl}_2/\text{hexane}$ 1/3(V/V) as eluent.

29 mg of **1** was obtained as yellow powder in a yield of 62%. mp: $194\text{--}196^\circ\text{C}$. ^1H NMR (CDCl_3) δ (ppm): 9.43–9.48 (m, 4H), 9.00 (d, $J = 7.6$ Hz, 2H), 8.01 (t, $J = 7.6$ Hz, 2H), 7.65 (t, $J = 7.6$ Hz, 2H), 7.59 (d, $J = 6.8$ Hz, 2H), 7.16 (s, 2H), 4.39–4.44 (m, 2H), 4.27–4.33 (m, 2H), 4.15–4.20 (m, 4H), 4.09 (d, $J = 12.0$ Hz, 1H), 3.72 (d, $J = 12.0$ Hz, 1H), 1.33–2.10 (m, 32H), 0.94 (t, $J = 7.2$ Hz, 6H), 0.87 (t, $J = 7.2$ Hz, 6H). ^{13}C NMR (CDCl_3) δ (ppm): 156.2, 156.18, 141.2, 131.2, 130.3, 129.0, 128.7, 128.1, 127.6, 126.4, 126.0, 124.8, 124.4, 123.9, 123.4, 123.1, 119.8, 119.4, 112.2, 110.0, 99.8, 70.4, 69.6, 43.5, 31.8, 31.7, 29.7, 29.6, 26.2, 26.1, 22.8, 22.7, 14.2, 14.1. HRMS (EI^+): calcd. for $\text{C}_{67}\text{H}_{68}\text{O}_4$ ($[\text{M}]^+$): 936.5112, found: 938.5106.

18 mg by-product **9** was isolated as brown powder in a yield of 37%. ^1H NMR (CDCl_3) δ (ppm): 9.43-9.50 (m, 4H), 9.02 (d, $J = 7.6$ Hz, 2H), 8.03 (t, $J = 8.0$ Hz, 2H), 7.83 (d, $J = 7.2$ Hz, 1H), 7.69 (m, 2H), 7.16 (d, $J = 8.0$ Hz, 2H), 4.77 (d, $J = 12.0$ Hz, 1H), 4.41-4.47 (m, 2H), 4.31-4.36 (m, 2H), 4.13-4.22 (m, 4H), 3.36 (d, $J = 12.0$ Hz, 1H), 1.25-2.11 (m, 32H), 0.94 (t, $J = 6.8$ Hz, 6H), 0.87 (t, $J = 6.8$ Hz, 6H). HRMS (EI^+): calcd. for $\text{C}_{67}\text{H}_{67}\text{ClO}_4$ ($[\text{M}]^+$): 970.4722, found: 970.4732.

Scheme S3 Synthesis of precursors **6** and **7**.



Tetraaryl-9H-tribenzo[a,c,e] cycloheptenes **6** and **7** were synthesized from **14** and **15**, respectively, in a way similar to the synthesis of **5**.

14: Yield: 81%. mp: 201-202 °C. ^1H NMR (CDCl_3) δ (ppm): 7.15-7.23 (m, 10H), 6.92 (d, $J = 6.8$ Hz, 4H), 6.77 (d, $J = 8.8$ Hz, 4H), 3.78 (s, 6H). ^{13}C NMR (CDCl_3) δ (ppm): 201.5, 159.1, 153.3, 133.7, 131.5, 129.5, 128.4, 128.1, 124.6, 123.5, 113.8, 55.3. HRMS (EI^+): calcd. for $\text{C}_{31}\text{H}_{24}\text{O}_3$ ($[\text{M}]^+$): 444.1720, found: 444.1723.

15: Yield: 77%. mp: 264-266 °C. ^1H NMR (CDCl_3) δ (ppm): 7.18 (d, $J = 8.8$ Hz, 4H), 6.85 (d, $J = 8.8$ Hz, 4H), 6.78 (d, $J = 8.8$ Hz, 4H), 6.71 (d, $J = 8.8$ Hz, 4H), 3.79 (s, 12H). ^{13}C NMR (CDCl_3) δ (ppm): 201.4, 159.7, 158.9, 152.9, 131.5, 131.2, 125.9, 124.1, 123.9, 113.8, 113.5, 55.3. HRMS (EI^+): calcd. for $\text{C}_{33}\text{H}_{28}\text{O}_5$ ($[\text{M}]^+$): 504.1931, found: 504.1928.

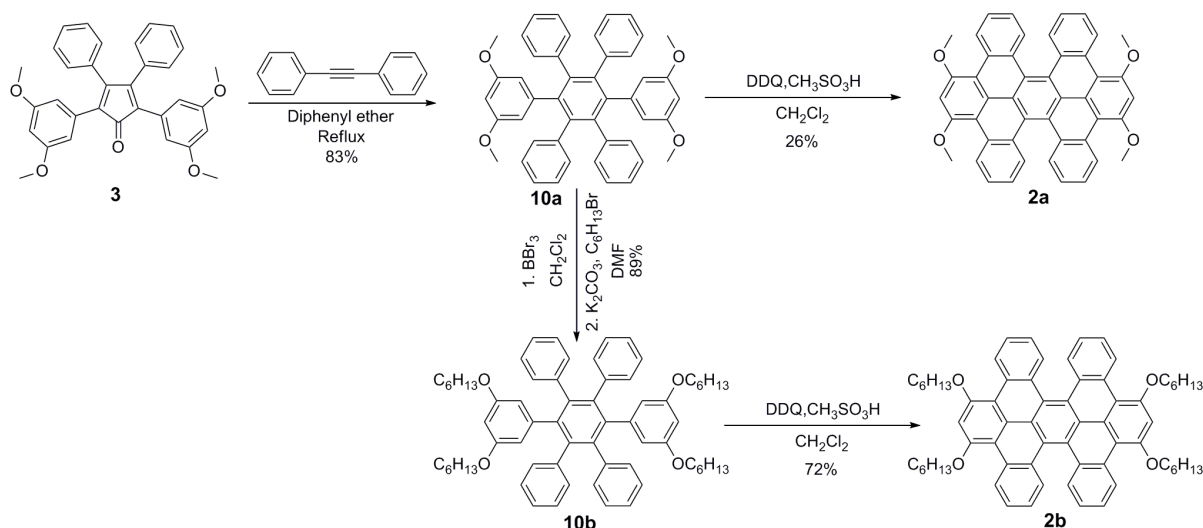
16: Yield: 12%. mp: sublimation before melting. ^1H NMR (CDCl_3) δ (ppm): 7.38 (d, $J = 7.6$ Hz, 2H), 7.16 (d, $J = 7.6$ Hz, 2H), 7.02 (m, 4H), 6.90 (t, $J = 7.6$ Hz, 2H), 6.79 (m, 4H), 6.69 (t, $J = 7.6$ Hz, 2H), 6.60 (t, $J = 7.6$ Hz, 2H), 6.45 (m, 6H), 6.36 (m, 2H), 4.14 (d, $J = 12.4$ Hz, 1H), 3.64 (d, $J = 12.4$ Hz, 1H), 3.62 (s, 6H). ^{13}C NMR (CDCl_3) δ (ppm): 157.2, 144.8, 141.9, 141.0, 139.9, 138.1, 135.9, 133.7, 133.1, 132.1, 132.1, 130.5, 127.0, 126.7, 126.1, 125.4, 125.1, 124.6, 112.5, 112.1, 55.1, 40.8. HRMS (EI^+): calcd. for $\text{C}_{45}\text{H}_{34}\text{O}_2$ ($[\text{M}]^+$): 606.2553, found: 606.2537.

17: Yield: 11%. mp: higher than 400 °C. ^1H NMR (CDCl_3) δ (ppm): 7.25 (d, $J = 7.6$ Hz, 2H), 7.15 (d, $J = 7.6$ Hz, 2H), 7.02 (d, $J = 7.6$ Hz, 2H), 6.89 (t, $J = 7.6$ Hz, 2H), 6.81 (d, $J = 7.6$ Hz, 2H), 6.59 (t, $J = 7.6$ Hz, 4H), 6.50 (d, $J = 7.6$ Hz, 2H), 6.43 (d, $J = 7.6$ Hz, 2H), 6.35 (m, 4H), 6.25 (dt, $J_1 = 7.6$ Hz, $J_2 = 2.4$ Hz, 2H), 4.12 (d, $J = 12.0$ Hz, 1H), 3.61-3.63 (m, 13H). ^{13}C NMR (CDCl_3) δ (ppm): 157.2, 157.0, 144.8, 142.0, 140.3, 138.0, 136.1, 134.0, 133.7, 133.1, 133.0, 132.1, 131.5, 126.6, 125.0, 124.6, 112.5, 112.4, 112.2, 111.8, 55.1, 55.0, 40.8. HRMS (EI^+): calcd. for $\text{C}_{47}\text{H}_{38}\text{O}_4$ ($[\text{M}]^+$): 666.2765, found: 666.2735.

6: Yield: 33%. mp: 211-212 °C. ^1H NMR (CDCl_3) δ (ppm): 7.37 (d, $J = 7.6$ Hz, 2H), 7.16 (d, $J = 7.6$ Hz, 2H), 7.01 (t, $J = 7.6$ Hz, 4H), 6.90 (t, $J = 7.6$ Hz, 2H), 6.79 (m, 4H), 6.69 (t, $J = 7.6$ Hz, 2H), 6.60 (t, $J = 7.2$ Hz, 2H), 6.41 (m, 6H), 6.35 (m, 2H), 4.13 (d, $J = 12.4$ Hz, 1H), 3.73 (dt, $J_1 = 6.4$ Hz, $J_2 = 2.0$ Hz, 4H), 3.64 (d, $J = 12.4$ Hz, 1H), 1.61 (m, 4H), 1.28 (m, 12H), 0.86 (t, $J = 6.4$ Hz, 6H). ^{13}C NMR (CDCl_3) δ (ppm): 156.7, 144.8, 141.9, 141.0, 139.9, 138.1, 136.0, 133.6, 133.5, 133.1, 132.2, 132.1, 130.5, 127.0, 126.6, 126.1, 125.4, 125.0, 124.6, 113.3, 112.8, 67.8, 40.8, 31.8, 29.3, 25.8, 22.7, 14.2. HRMS (EI^+): calcd. for $\text{C}_{55}\text{H}_{54}\text{O}_2$ ($[\text{M}]^+$): 746.4118, found: 746.4154.

7: Yield: 23%. mp: 57-58 °C. ^1H NMR (CDCl_3) δ (ppm): 7.22 (dt, $J_1 = 8.4$ Hz, $J_2 = 2.4$ Hz, 2H), 7.14 (d, $J = 7.6$ Hz, 2H), 6.99 (d, $J = 8.0$ Hz, 2H), 6.88 (t, $J = 7.6$ Hz, 2H), 6.80 (d, $J = 7.6$ Hz, 2H), 6.57 (m, 4H), 6.48 (d, $J = 8.4$ Hz, 2H), 6.40 (d, $J = 7.6$ Hz, 2H), 6.32 (m, 4H), 6.24 (dt, $J_1 = 8.4$ Hz, $J_2 = 2.4$ Hz, 2H), 4.11 (d, $J = 12.4$ Hz, 1H), 3.72-3.78 (m, 8H), 3.61 (d, $J = 12.4$ Hz, 1H), 1.63-1.68 (m, 8H), 1.30-1.37 (m, 24H), 0.87-0.90 (m, 12H). ^{13}C NMR (CDCl_3) δ (ppm): 156.7, 156.6, 144.8, 142.1, 140.3, 137.9, 136.2, 133.8, 133.7, 133.5, 133.2, 133.0, 132.1, 131.5, 126.5, 125.0, 124.6, 113.2, 113.1, 112.9, 112.5, 67.9, 67.8, 40.8, 31.8, 29.4, 29.3, 25.8, 22.7, 14.2. HRMS (EI^+): calcd. for $\text{C}_{67}\text{H}_{78}\text{O}_4$ ($[\text{M}]^+$): 946.5895, found: 946.5883.

Scheme S4 Synthesis of **2a** and **2b**.



1,4-Bis(3,5-dimethoxyphenyl)-2,3,5,6-tetraphenylbenzene (**10a**)

A suspension of 2,5-bis(3,5-dimethoxyphenyl)-3,4-diphenylcyclopentadienone (**3**) (504 mg, 1 mmol) and diphenylacetylene (196 mg, 1.1 mmol) in 3 ml of diphenylether was heated to reflux overnight under a N_2 atmosphere. The solution was cooled to room temperature and poured into 100 ml of cooled methanol. The resulting brownish powders were filtered and purified by column chromatography on silica gel with CH_2Cl_2 /hexane 1/1(V/V) as eluent.

546 mg of **10a** was collected as white powder in a yield of 83%. mp: 383-384 °C. ¹H NMR (CDCl₃) δ (ppm): 6.88 (m, 20H), 5.98 (m, 6H), 3.40 (s, 12H). ¹³C NMR (CDCl₃) δ (ppm): 159.3, 142.3, 140.8, 140.4, 131.4, 126.9, 125.5, 110.3, 99.2, 55.3. HRMS (EI⁺): calcd. for C₄₆H₃₈O₄ ([M]⁺): 655.2843, found: 655.2842.

1,4-Bis(3,5-dihexyloxyphenyl)-2, 3,5,6-tetraphenylbenzene (10b)

To a solution of **10a** (490 mg, 0.75 mmol) in 50 ml of anhydrous CH₂Cl₂ was added a solution of BBr₃ (15 ml, 1M in CH₂Cl₂) at 0 °C under an atmosphere of nitrogen. The solution was warmed to room temperature and heated to reflux for 4 hours. Then the reaction mixture was cooled with ice bath and quenched with H₂O. The mixture was extracted with diethyl ether, washed with water and brine, dried with anhydrous Na₂SO₄, and concentrated under reduced pressure. The crude product of 1,4-bis(3,5-dihydroxyphenyl)-2,3,5,6-tetraphenylbenzene was collected as light yellow powders and used in the next step without further purification.

To a suspension of crude 1,4-bis(3,5-dihydroxyphenyl)-2,3,5,6-tetraphenylbenzene and K₂CO₃ (2.07 g, 15 mmol) in 5 ml of DMF was added 2.1 ml of bromohexane (1.47 g, 15 mmol). The solution was heated at 85 °C under an atmosphere of nitrogen overnight. Then the reaction mixture was diluted with water, extracted with diethyl ether. The ether extracts were washed with water and brine, dried with anhydrous Na₂SO₄, and then concentrated under reduced pressure. The resulting crude product was purified by column chromatography on silica gel with CH₂Cl₂/hexane 1/2 (V/V) as eluent yielding 625 mg (89%) of **10b** as white powders. mp: 121-122 °C. ¹H NMR (CDCl₃) δ (ppm): 6.86 (m, 20H), 5.97 (m, 6H), 3.48 (t, *J* = 6.8 Hz, 8H), 1.49 (m, 8H), 1.23-1.32 (m, 24H), 0.87 (t, *J* = 6.8 Hz, 12H). ¹³C NMR (CDCl₃) δ (ppm): 158.8, 142.1, 140.9, 140.4, 140.3, 131.4, 126.8, 125.4, 111.1, 101.0, 68.3, 31.6, 29.1, 25.7, 22.7, 14.2. HRMS (EI⁺): calcd. for C₆₆H₇₈O₄ ([M+H]⁺): 935.5973, found: 935.5967.

1,3,12,14-tetrahexyloxyhexabenz[*a,cd,f,j,lm,o*]perylene (HBP) (twisted-2b)

To a solution of **10b** (65 mg, 0.07 mmol) in 9 ml of anhydrous CH₂Cl₂ cooled at 0°C was added 1 ml of MeSO₃H and 76 mg of DDQ (0.33 mmol). The colourless solution of reaction mixture turned black gradually. The reaction was stirred at 0°C for 1 hour and then was quenched with an aqueous solution of NaHCO₃ and extracted with CH₂Cl₂. The organic layer was separated and washed with H₂O and brine, dried with anhydrous Na₂SO₄, then concentrated under reduced pressure. The resulting red solid was further purified by column chromatography on silica gel with CH₂Cl₂/hexane 1/2(V/V) as eluent yielding 47 mg of twisted-**2b** as red powders in a yield of 72%. mp: 223-225 °C (When the melting point of twisted-**2b** was measured with a differential scanning calorimeter (DSC) and a polarized light microscope that was equipped with a heating stage, two phase transitions at 214-215 °C and 223-225 °C were found. The phase transition at 214-215 °C likely corresponds to a transition from crystals to liquid crystals in accompany with thermal isomerization to anti-**2b**). ¹H NMR (CD₂Cl₂) δ (ppm): 9.56 (d, *J* = 8.4 Hz, 4H), 8.49 (d, *J* = 8.4 Hz, 2H), 7.42 (m, 6H), 7.14 (t, *J* = 7.6 Hz, 4H), 4.53-4.58 (m, 4H), 4.37-4.42 (m, 4H), 2.12-2.19 (m, 4H), 1.71-1.78 (m, 4H), 1.44-1.52(m, 16H), 0.97 (t, *J* = 7.2 Hz, 6H). ¹³C NMR (CDCl₃) δ (ppm): 158.1, 131.2, 131.1, 129.6, 128.3, 126.7, 126.3, 125.7, 125.3, 124.6, 113.5, 99.2, 70.3, 32.1, 30.0, 26.6, 23.1, 14.3. HRMS (EI⁺): calcd. for C₆₆H₇₀O₄ ([M]⁺): 926.5269, found: 926.5290.

1,3,12,14-tetramethoxyhexabenz[*a,cd,f,j,lm,o*]perylene (HBP) (2a)

2a was synthesized from 46 mg (0.07 mmol) of 1,4-Bis(3,5-dimethoxyphenyl)-2, 3,5,6-tetraphenylbenzene (**10a**) in a way similar to the synthesis of **2b**. 12 mg of **2a** was collected as red powders. Yield: 26%. mp: higher than 400 °C. ¹H NMR (CD₂Cl₂) δ (ppm): 9.47 (d, *J* = 8.4 Hz, 4H), 8.47 (d, *J* = 8.4 Hz, 4H), 7.42 (m, 6H), 7.14 (t, *J* = 7.6 Hz, 4H), 4.36

(s, 12H). Due to low solubility in common solvents, ^{13}C NMR spectrum of molecule **2a** was not recorded. HRMS (EI^+): calcd. for $\text{C}_{46}\text{H}_{30}\text{O}_4$ ($[\text{M}]^+$): 646.2139, found: 646.2139.

2. Variable temperature ^1H NMR for compounds **1** and **8**.

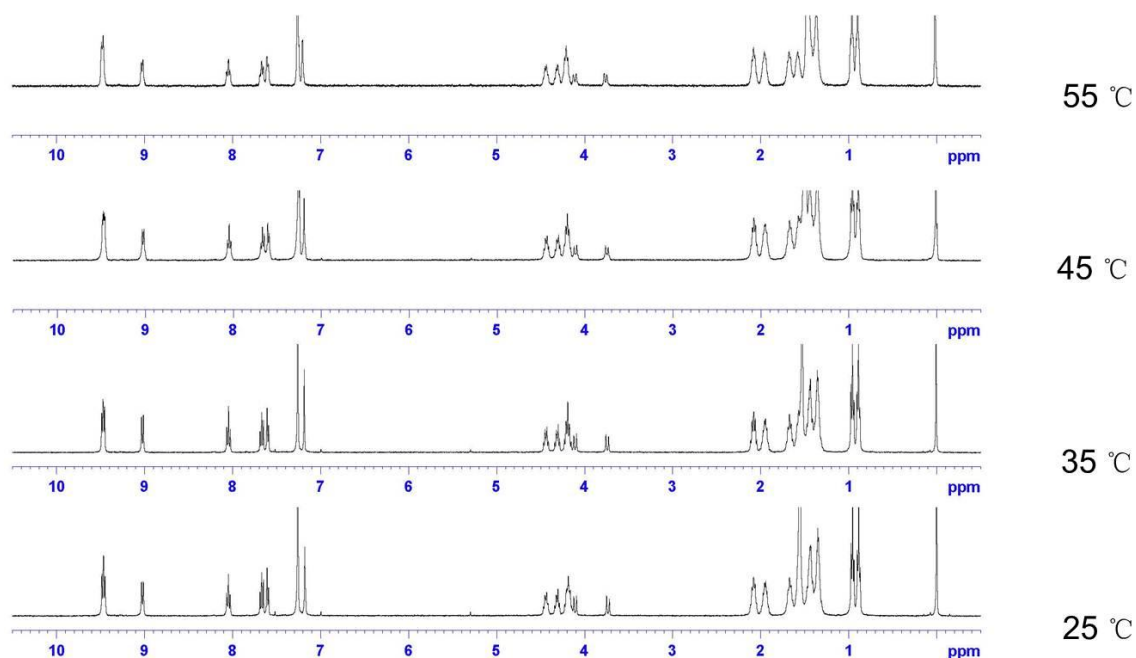


Figure S1 ^1H NMR of **1** in CDCl_3 as recorded at varied temperature.

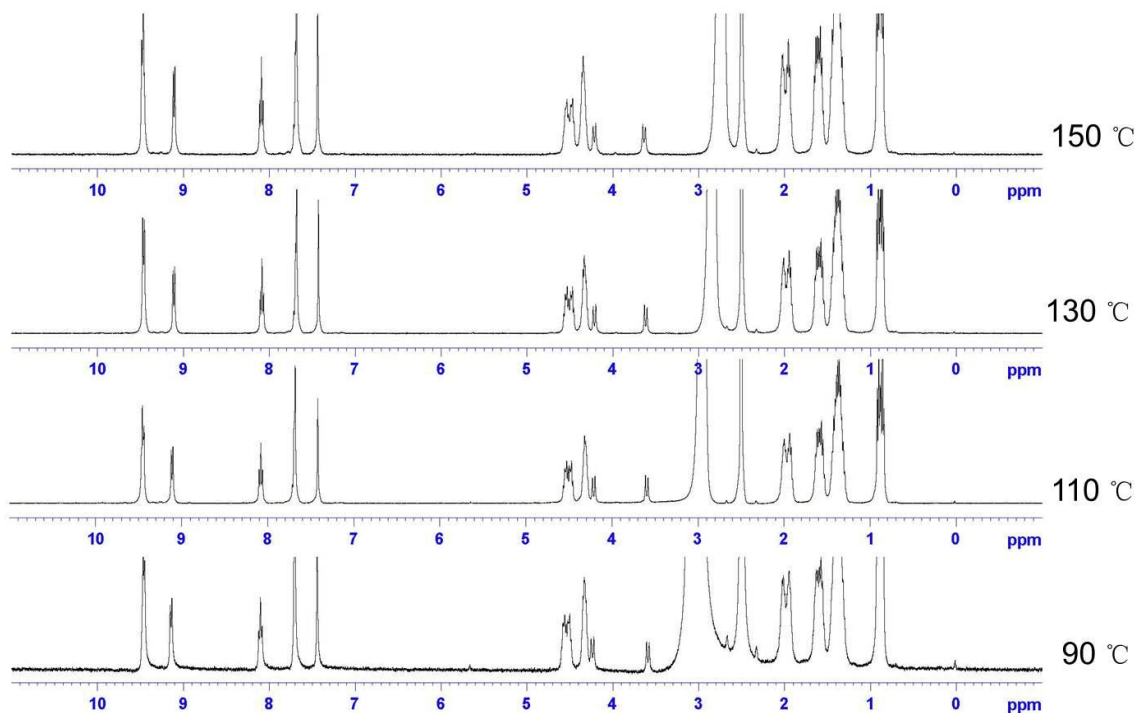


Figure S2 ^1H NMR of **1** in DMSO-d_6 as recorded at varied temperature.

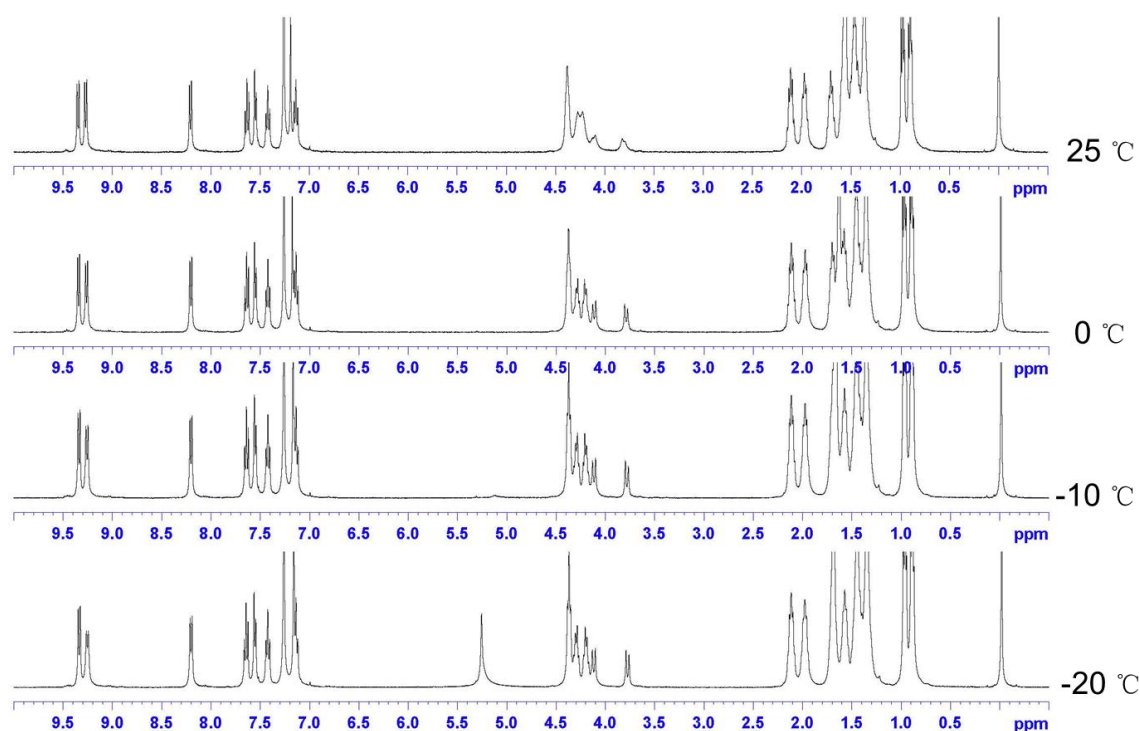


Figure S3 ^1H NMR of **8** in CDCl_3 as recorded at varied temperature.

3. Thermal isomerization of twisted-**2b** and *anti*-**2b**

10 mg of twisted-**2b** was dissolved in 2 ml of toluene and heated to reflux under N_2 for 1 hour. The resulting solution was cooled to room temperature and concentrated under reduced pressure. The powder obtained was further purified by column chromatography on silica gel with CH_2Cl_2 /hexane 1/3 (V/V) as eluent. 2 mg of *anti*-**2b** was obtained as yellow powder (yield 20%) and 6 mg red powder of twisted-**2b** was recycled. To improve the yield of the *anti*-**2b**, 10 mg of twisted-**2b** in 2 ml of toluene was heated to boil under N_2 without a condenser allowing the solvent to evaporate. From the concentrated solution, yellow powders precipitated. The suspension was cooled to room temperature, triturated with ethanol and filtered. The filtration residue was washed with 3×5 ml of ethanol yielding *anti*-**2b** as 8 mg yellow powders. mp: the surface of yellow crystallites started to turn red when heated above 200 °C indicating partial formation of twisted-**2b**, and the solids finally melted at 231-233 °C. ^1H NMR (CD_2Cl_2) δ (ppm): 9.15 (d, $J = 8.4$ Hz, 4H), 8.19 (d, $J = 8.4$ Hz, 2H), 7.40 (t, $J = 7.2$ Hz, 4H), 7.31 (s, 2H), 7.07 (t, $J = 7.2$ Hz, 4H), 4.48-4.54 (m, 4H), 4.38-4.43 (m, 4H), 2.10-2.15 (m, 8H), 0.97-1.76 (36H). ^{13}C NMR spectrum of molecule *anti*-**2b** was not recorded because of its low solubility in common solvents at a temperature low enough to avoid fast thermal isomerization. HRMS (EI^+): calcd. for $\text{C}_{66}\text{H}_{70}\text{O}_4$ ($[\text{M}]^+$): 926.5269, found: 926.5288.

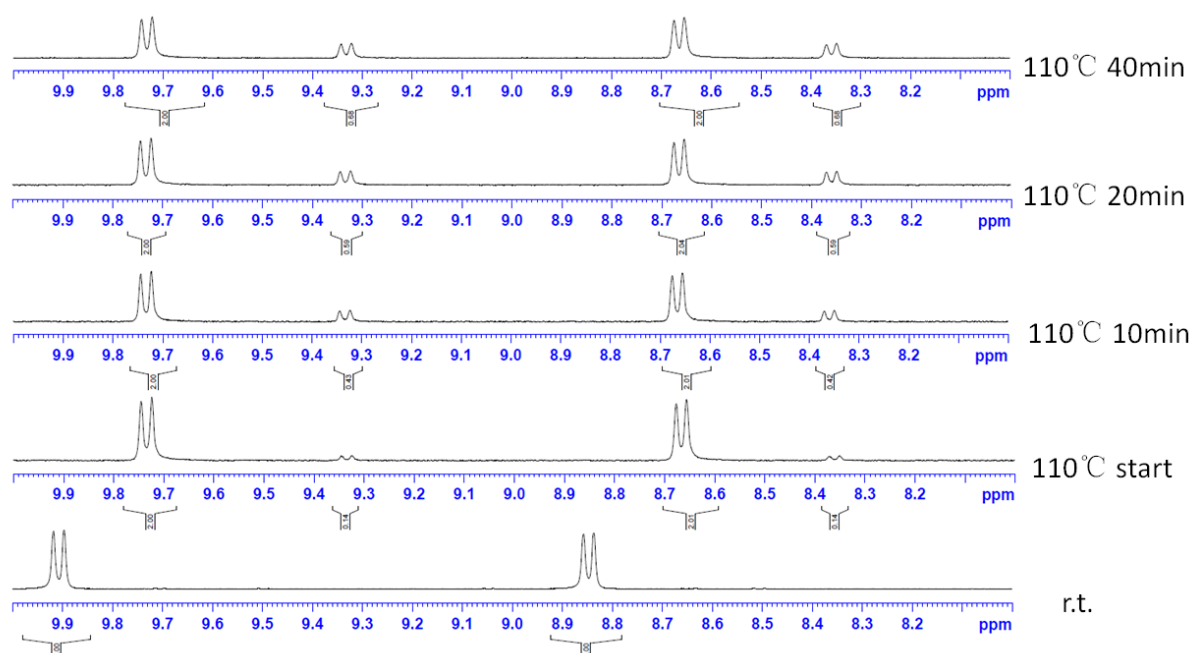


Figure S4 Selected ^1H NMR spectra of **2b** during the progress of thermal twisted-to-*anti* isomerization in toluene-d_8 at 110 °C.

4. UV-vis absorption spectra

All the UV-vis spectra were recorded at a concentration of $5 \times 10^{-6} \text{ mol/L}$.

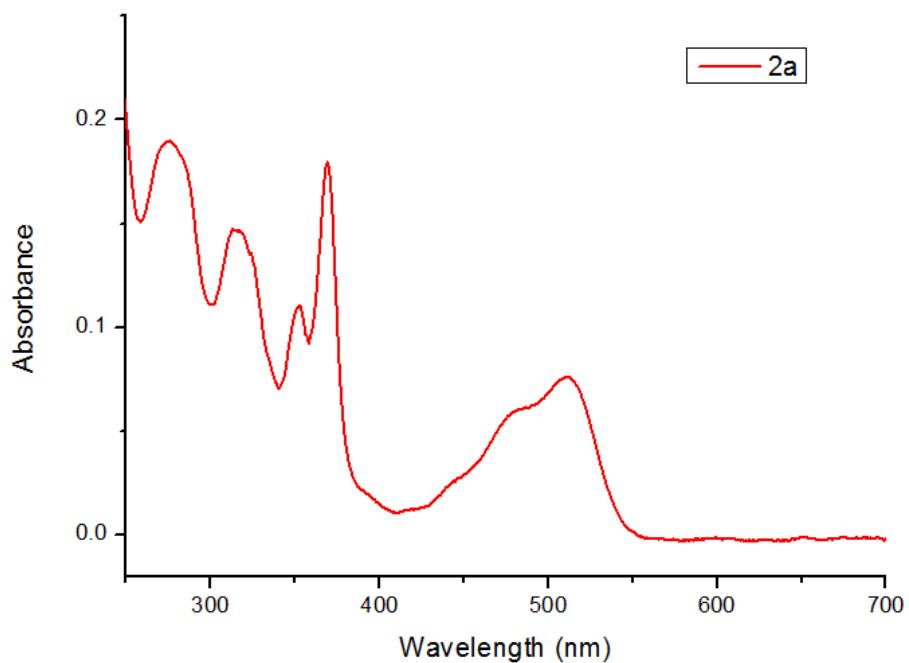


Figure S5 UV-vis absorption spectrum of twisted-**2a** in CH_2Cl_2

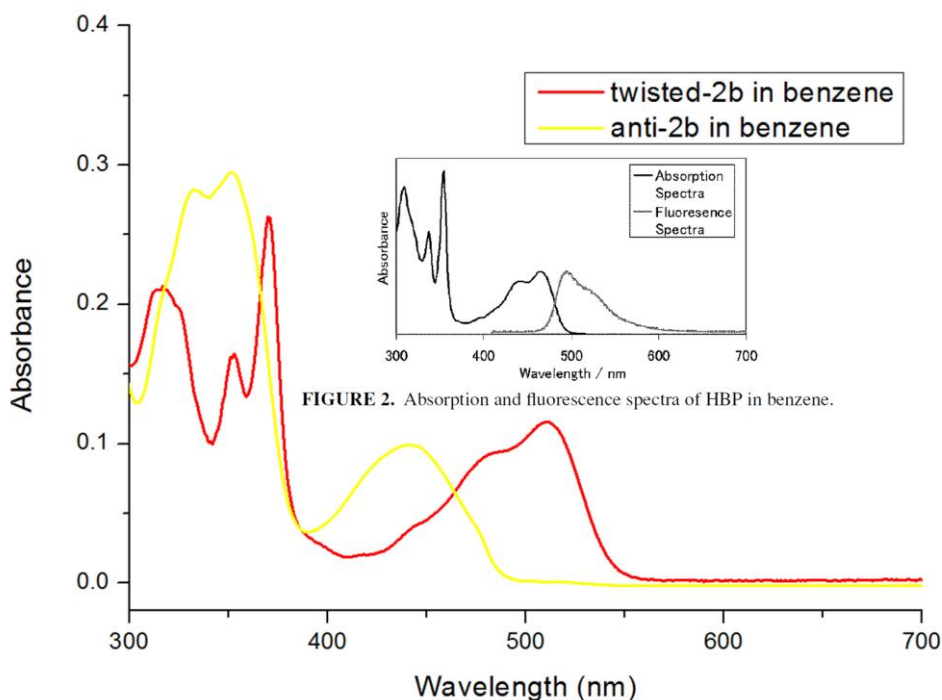


FIGURE 2. Absorption and fluorescence spectra of HBP in benzene.

Figure S6 UV-vis absorption spectra of twisted-**2b** (red trace) and *anti-2b* (yellow trace) in benzene. (Inset figure, which shows UV-vis absorption and fluorescence spectra of twisted-HBP in benzene, is copied from Ref. 2 with permission of Taylor & Francis. Copyright 2004.)

5. Density functional theory (DFT) Calculation

The molecules were optimized with the B3LYP/6-31G(d,p) basis set and the energy levels of HOMO and LUMO were calculated with the B3LYP/6-311++G(d,p) basis set using the Gaussian 09 software package.³ the energy levels of HOMO and LUMO was calculated with the 6-311++G(d,p) basis set.

2. Fujimaki, Y.; Takekawa, M.; Fujisawa, S.; Ohshima, S. Sakamoto, Y. *Polycyclic Aromatic Compounds*, **2004**, 24, 107–122.

3. Gaussian 09, Revision B.01, Frisch, M. J.; Trucks, G. W.; Schlegel, H. B.; Scuseria, G. E.; Robb, M. A.; Cheeseman, J. R.; Scalmani, G.; Barone, V.; Mennucci, B.; Petersson, G. A.; Nakatsuji, H.; Caricato, M.; Li, X.; Hratchian, H. P.; Izmaylov, A. F.; Bloino, J.; Zheng, G.; Sonnenberg, J. L.; Hada, M.; Ehara, M.; Toyota, K.; Fukuda, R.; Hasegawa, J.; Ishida, M.; Nakajima, T.; Honda, Y.; Kitao, O.; Nakai, H.; Vreven, T.; Montgomery, Jr., J. A.; Peralta, J. E.; Ogliaro, F.; Bearpark, M.; Heyd, J. J.; Brothers, E.; Kudin, K. N.; Staroverov, V. N.; Kobayashi, R.; Normand, J.; Raghavachari, K.; Rendell, A.; Burant, J. C.; Iyengar, S. S.; Tomasi, J.; Cossi, M.; Rega, N.; Millam, J. M.; Klene, M.; Knox, J. E.; Cross, J. B.; Bakken, V.; Adamo, C.; Jaramillo, J.; Gomperts, R.; Stratmann, R. E.; Yazyev, O.; Austin, A. J.; Cammi, R.; Pomelli, C.; Ochterski, J. W.; Martin, R. L.; Morokuma, K.; Zakrzewski, V. G.; Voth, G. A.; Salvador, P.; Dannenberg, J. J.; Dapprich, S.; Daniels, A. D.; Farkas, Ö.; Foresman, J. B.; Ortiz, J. V.; Cioslowski, J.; Fox, D. J. Gaussian, Inc., Wallingford CT, 2009.

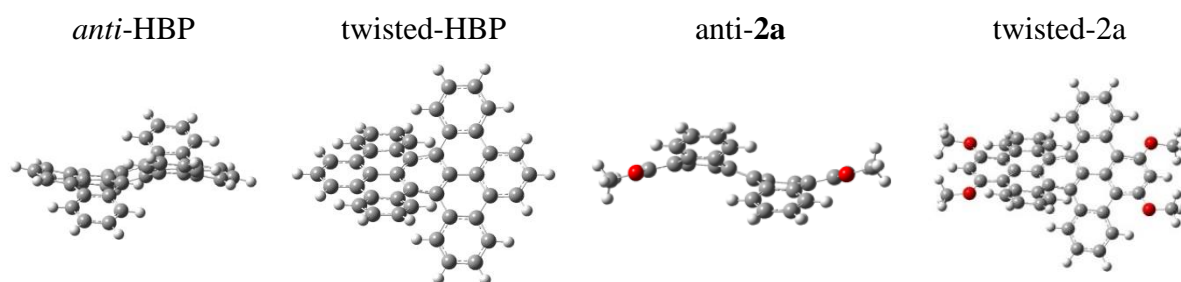


Figure S7 Energy-minimized models for *anti*-HBP, twisted-HBP, *anti*-2a and twisted-2a.

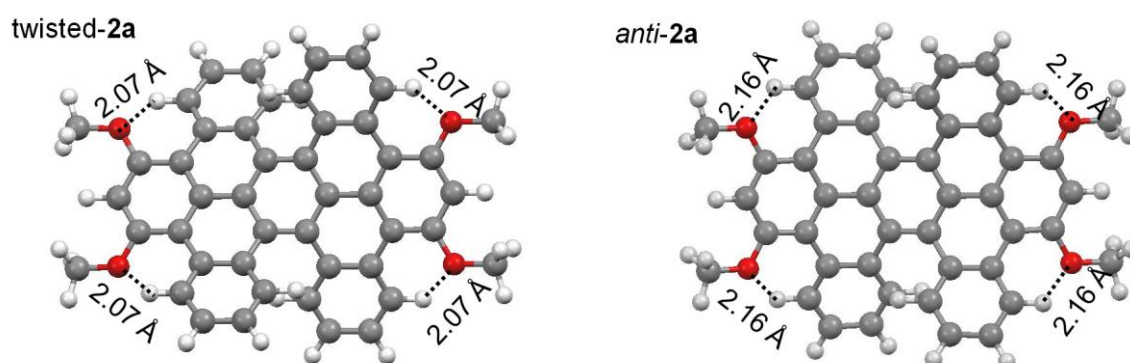


Figure S8 Energy-minimized models for twisted-2a and *anti*-2a showing the distance between oxygen atoms and neighboring aromatic hydrogen atoms.

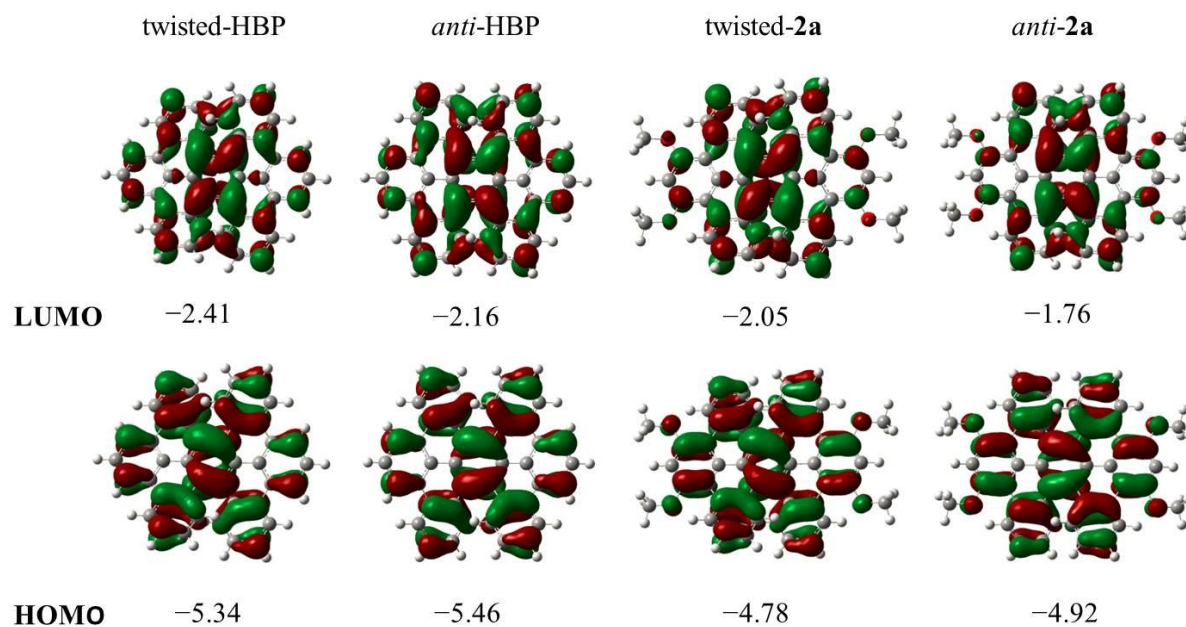


Figure S9 Calculated frontier molecular orbitals of HBP and 2a with the energy levels.

6. Cyclic Voltammetry

The cyclic voltammetry was performed in a solution of DCM with 0.1M Bu₄NPF₆ as the supporting electrolyte, at a scan rate of 50mVs⁻¹. Ferrocene/ferrocenium was used as the internal standard. Potentials were referenced to ferrocenium/ferrocene (FeCp₂⁺/FeCp₂⁰).

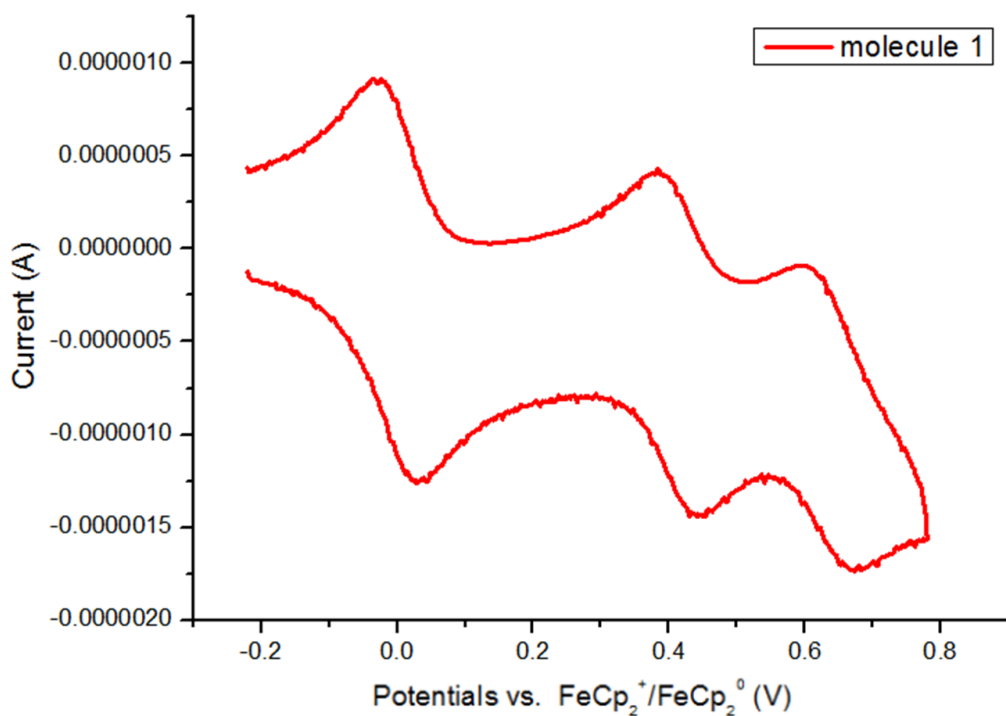


Figure S10 Cyclic voltammogram of **1**

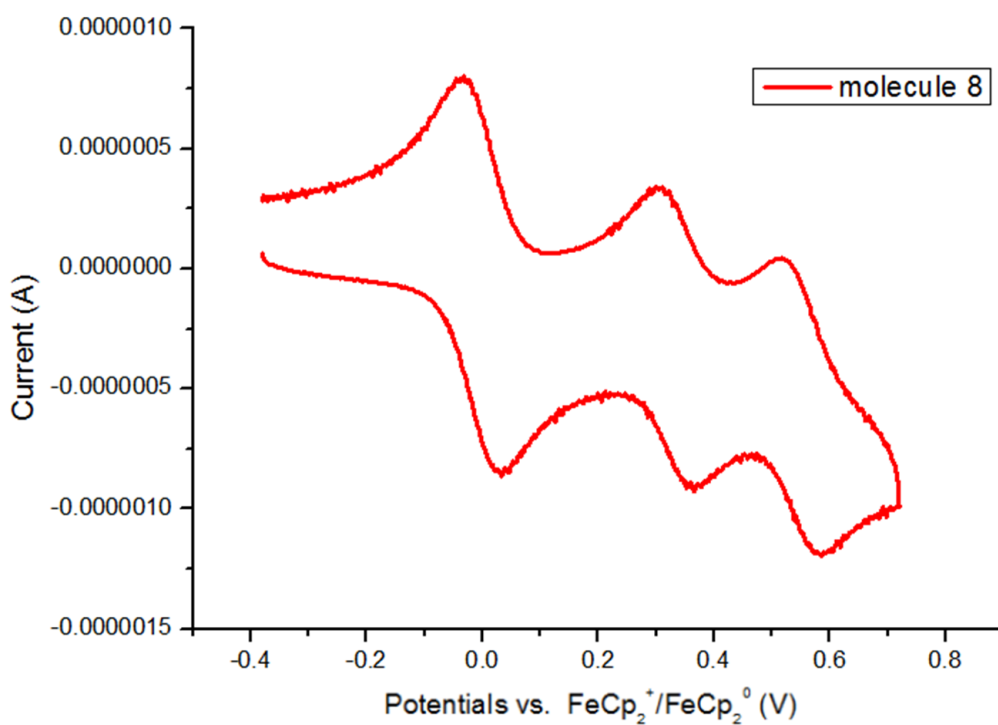


Figure S11 Cyclic voltammogram of **8**

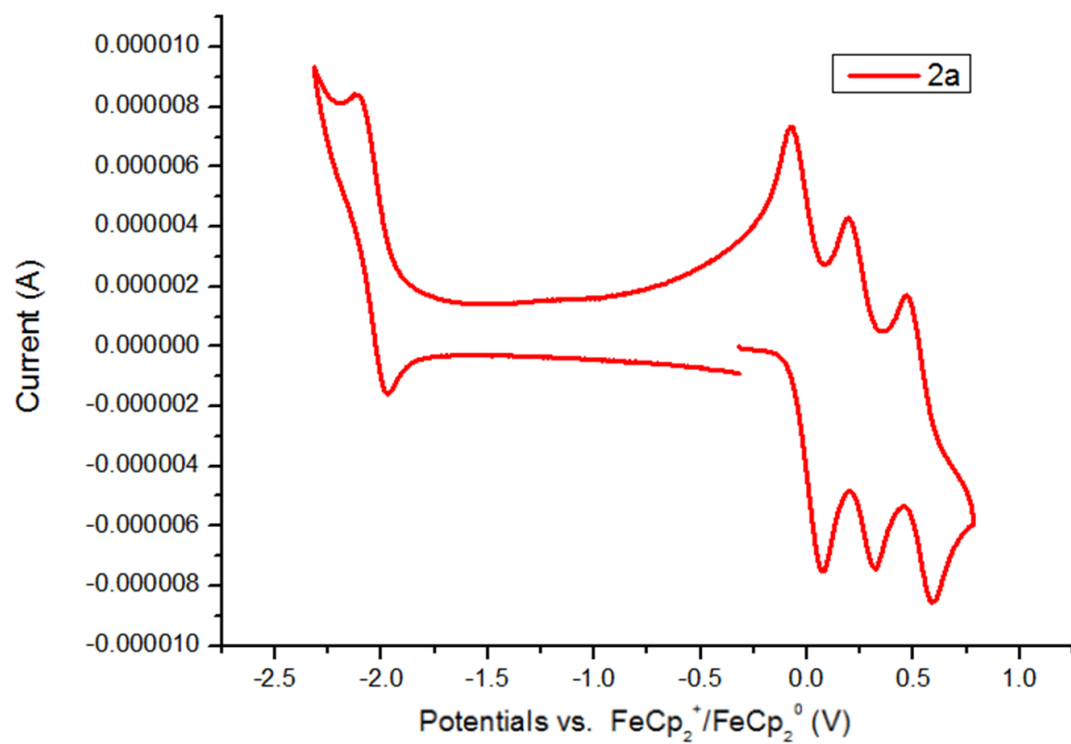


Figure S12 Cyclic voltammogram of twisted-2a

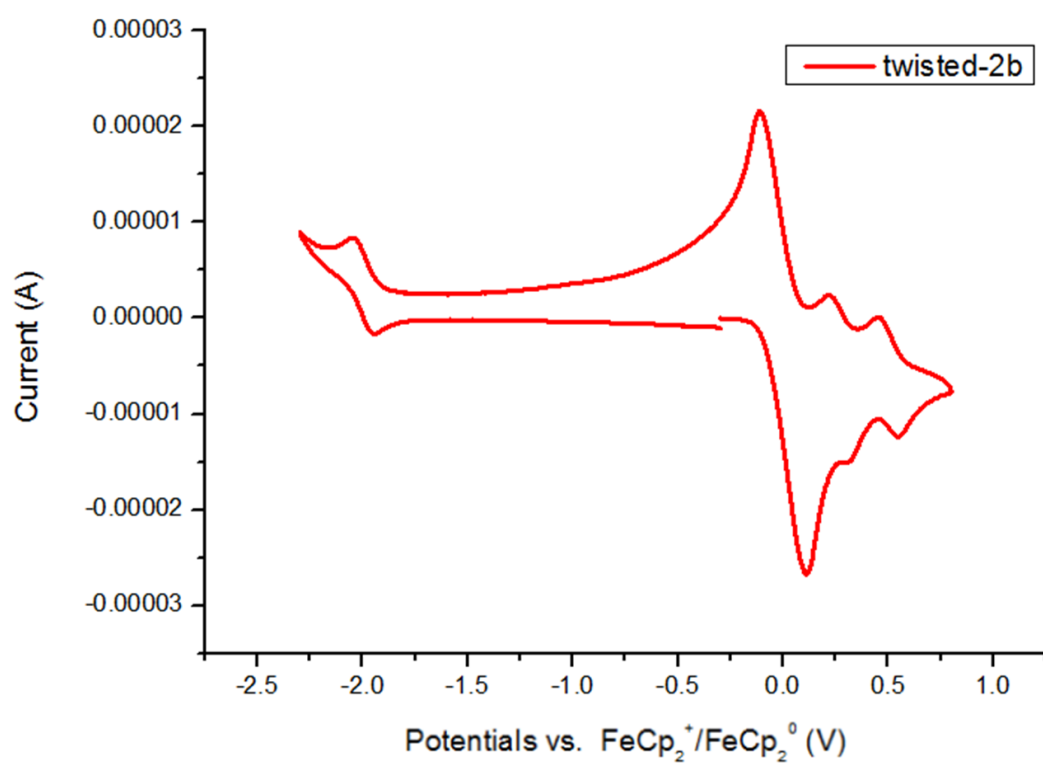


Figure S13 Cyclic voltammogram of twisted-2b

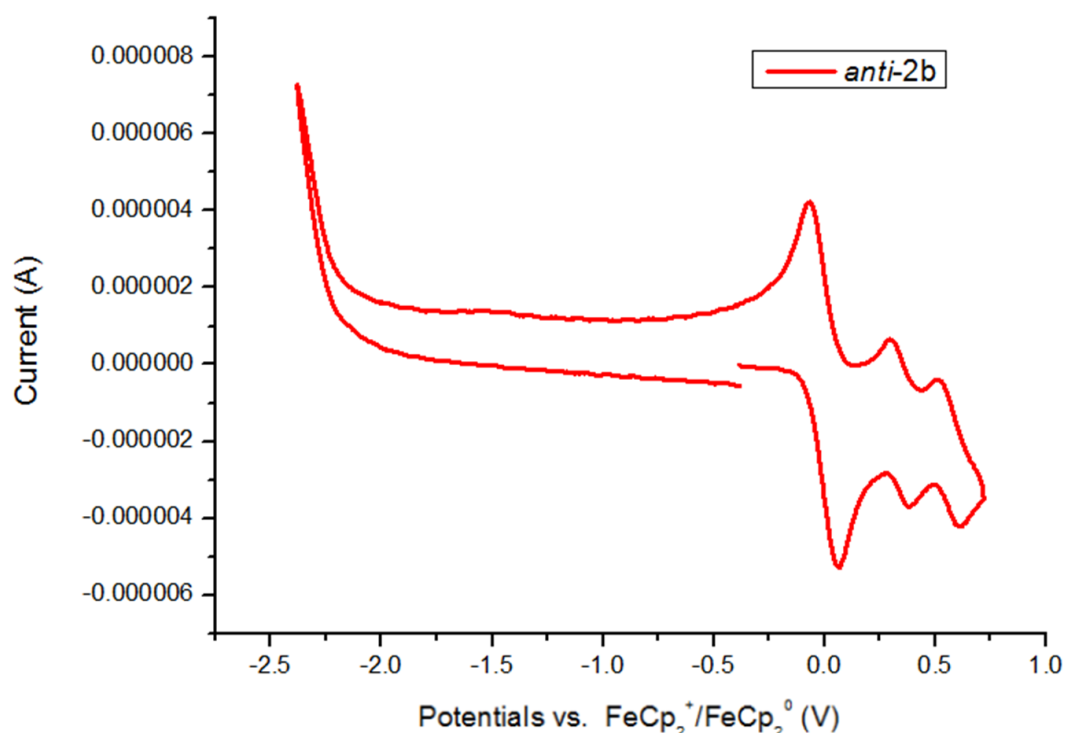


Figure S14 Cyclic voltammogram of *anti-2b*

Table S1 Summary of electrochemical potentials and energy levels of LUMO and HOMO

Compound	Reduction potential vs Fc^+/Fc (V)	Oxidation potential vs Fc^+/Fc (V)		HOMO (eV)	LUMO (eV)
		E_{ox1}	E_{ox2}		
1	/	0.41	0.64	-5.21	/
8	/	0.33	0.55	-5.13	/
twisted- 2a	-2.04	0.25	0.53	-5.05	-2.76
twisted- 2b	-2.04	0.22	0.50	-5.02	-2.76
<i>anti-2b</i>	/	0.34	0.57	-5.14	/

7. Fabrication and characterization of solution-processed thin films and transistors

(1) Deposition of thin films and fabrication of transistors

Silicon wafers used for fabrication of thin film transistors had 300 nm-thick SiO_2 on highly n-doped Si, and were cleaned with the following treatments: soaked in a solution of 70:30 $\text{H}_2\text{SO}_4/\text{H}_2\text{O}_2$ (piranha) for 1 hour at 100 °C, rinsed with deionized water and finally treated with oxygen plasma. To form bottom-contact drain and source electrodes, 40 nm-thick gold with a 2 nm-thick chromium adhesive layer was vacuum-deposited through a shadow mask onto the pretreated wafer, by using an Edwards Auto 306 vacuum coater with a Turbomolecular pump at a pressure of 4.0×10^{-6} torr or lower, with a deposition rate of ca. 2 Å/s to desired thickness. The gold electrode surface was then treated with a 10 mM solution of pentafluorobenzenethiol (PFBT) in toluene for 2 minutes following the reported

procedure.⁴ Then the SiO₂ dielectric surface was treated with hexamethyldisilazane (HMDS) by spin-coating neat HMDS at 4000 rpm onto the SiO₂/Si wafer that had bottom-contact PFBT-modified gold electrodes following the reported procedure.⁴ The resulting HMDS-modified SiO₂ surface had a water contact angle of about 60°. Thin films of **1**, twisted-**2b** and *anti*-**2b** were deposited by drop-casting a 1 wt% solution of one of these compounds in chlorobenzene onto the HMDS modified SiO₂/Si wafer, which was heated at 60 °C by a heating stage in ambient. The resulting semiconducting channels had dimensions of 50µm(L)×1mm(W), 100µm(L)×1mm(W), 150µm(L)×1mm(W), 50µm(L)×2mm(W) and 100µm(L)×2mm(W). After deposition of organic films, the devices were annealed under room temperature in solvent-rich ambient for 60 minutes and then placed in a vacuum oven at 90 °C overnight to totally remove the organic solvent.

(2) Characterization of Thin Film Transistors

X-ray diffraction (XRD): XRD data were recorded on a SmartLab X-Ray Refractometer of the thin films deposited by solution based process.

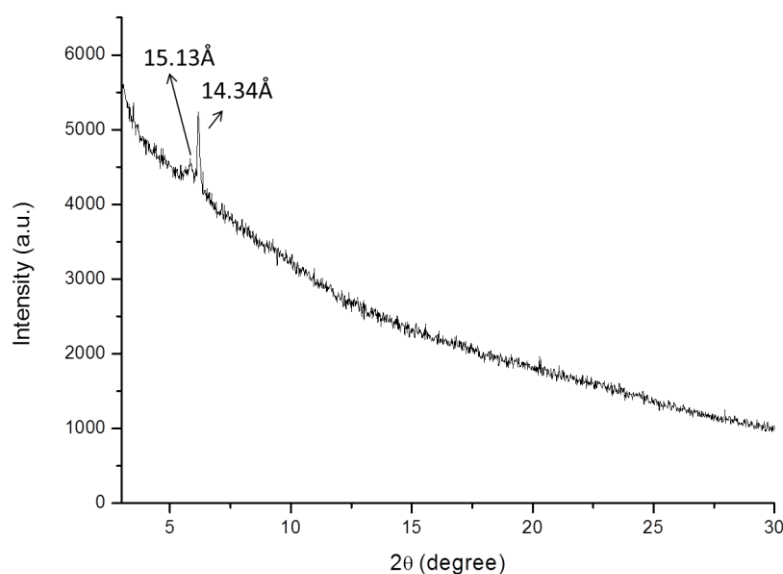


Figure S15 X-ray diffraction from thin film of twisted-**2b** by solution process with the substrate of 60°C (deposited by drop-casting from 1wt% chlorobenzene solution).

4. Park, S. K.; Jackson, T. N.; Anthony, J. E.; Mourey, D. A.; *Appl. Phys. Lett.* **2007**, *91*, 063514.

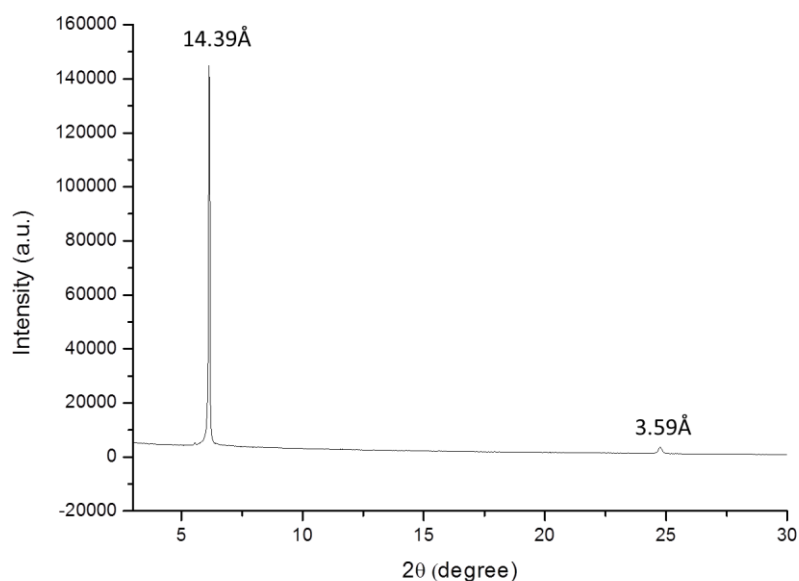


Figure S16 X-ray diffraction from thin film of *anti-2b* by solution process.

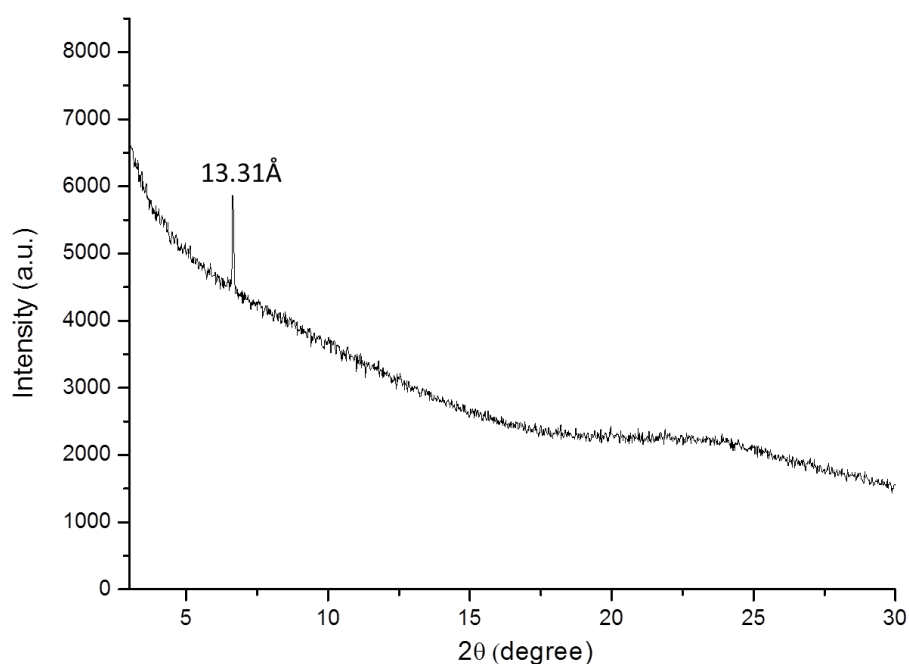


Figure S17 X-ray diffraction from thin film of **1** by solution process.

Atomic Force Microscopy (AFM): Thin films deposited through solution process were used for AFM studies. The topographic images were obtained using a Nanoscope IIIa Multimode Microscope from Digital Instruments, using tapping mode and in air under ambient condition. The topographic images were collected from multiple samples, and for each sample, different regions were scanned to ensure reproducibility.

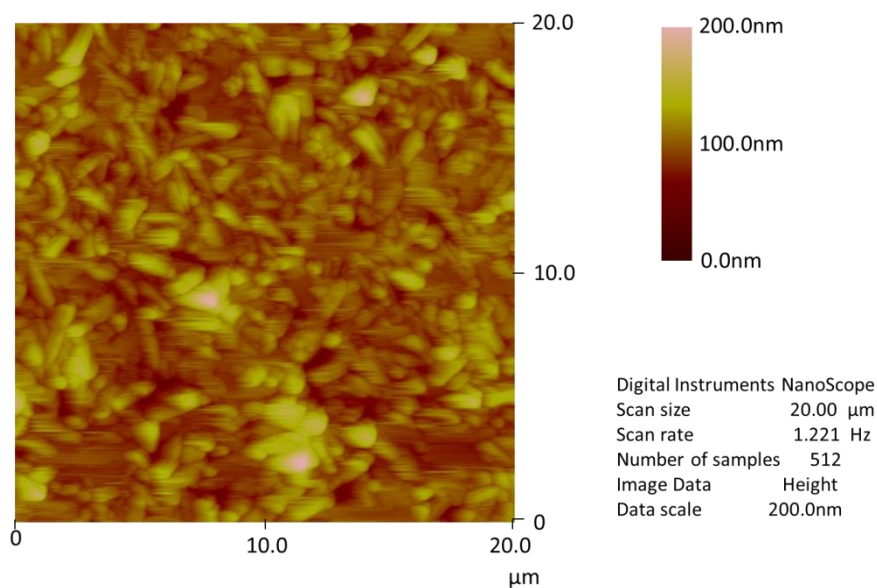


Figure S18 AFM images from thin film of twisted-**2b** (1wt% chlorobenzene solution deposited onto HMDS modified SiO₂/Si wafer under 60 °C)

(3) Electrical Characterization of Thin Film Transistors

The current-voltage measurement was carried out on a JANIS ST-500-20-4TX probe station with a Keithley 4200 Semiconductor Characterization System at room temperature in ambient air. Results showed that twisted-**2b** performed as p-channel transistors with a field effect mobility of 5×10^{-5} to $2 \times 10^{-4} \text{ cm}^2 \text{ V}^{-1} \text{ s}^{-1}$.

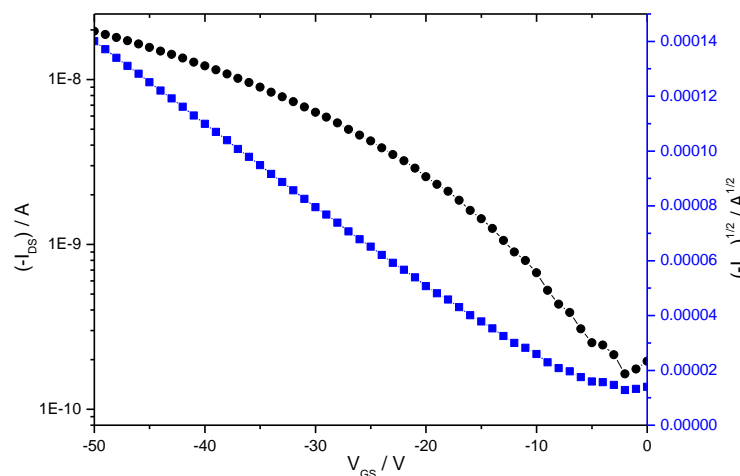
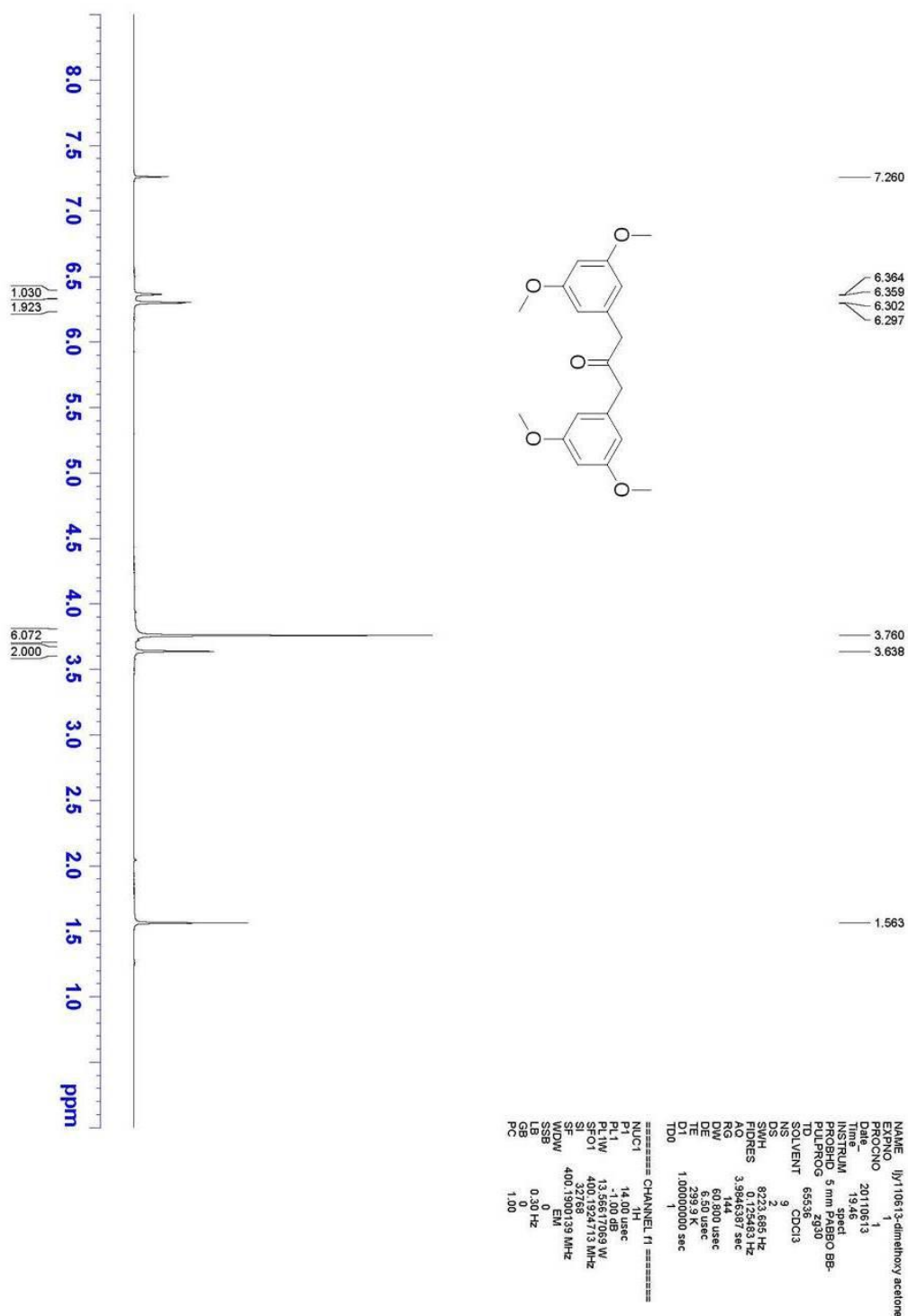
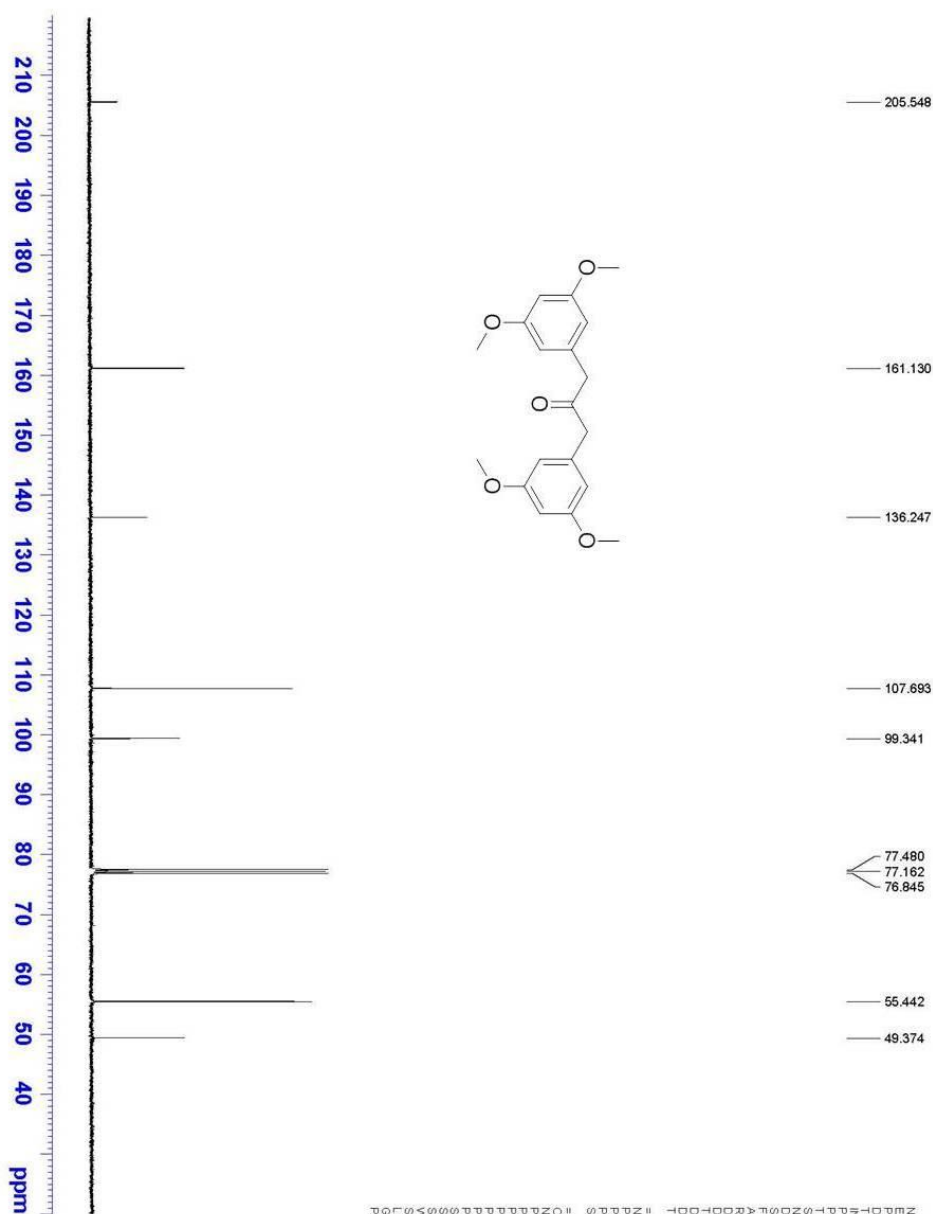


Figure S19 Typical transfer curves of thin film transistor of twisted-**2b** deposited on HMDS-treated SiO₂ at a substrate temperature of 60 °C with channel 50 μm(L)×1 mm(W) showing a hole mobility of $1.04 \times 10^{-4} \text{ cm}^2/\text{V} \cdot \text{s}$ (tested in the air).

8. NMR spectra



¹H NMR spectrum of **12**



```

NAME | \j710716-diphenyl acetone C13
EXPNO | 1
PROCNO | 1
Date_ | 20110716
Time | 12.11.11
INSTRUM | spect
PROBHD | 5mm PABBO BB-
PULPROG | zgpg30
TD | 65536
SOLVENT | CDCl3
DS | 362
NS | 544
DSH | 24038.451 Hz
F2PRES | 0.366788 Hz
RG | 1.321668 sec
DWT | 20.600 usec
TE | 300.2 K
D1 | 2.00000000 sec
D11 | 0.03000000 sec
TD0 | 1

===== CHANNEL f1 =====
NUC1 | 13C
P1 | 9.00 usec
PL1 | -2.00 dB
SFO1 | 100.627183 MHz

===== CHANNEL f2 =====
NUC2 | 1H
P2 | 12.00 usec
PL2 | -1.00 dB
SFO2 | 400.151993 MHz

===== CHANNEL f3 =====
NUC3 | 1H
P3 | 12.00 usec
PL3 | -1.00 dB
SFO3 | 400.151993 MHz

===== CHANNEL f4 =====
NUC4 | 1H
P4 | 12.00 usec
PL4 | -1.00 dB
SFO4 | 400.151993 MHz

===== CHANNEL f5 =====
NUC5 | 1H
P5 | 12.00 usec
PL5 | -1.00 dB
SFO5 | 400.151993 MHz

===== CHANNEL f6 =====
NUC6 | 1H
P6 | 12.00 usec
PL6 | -1.00 dB
SFO6 | 400.151993 MHz

===== CHANNEL f7 =====
NUC7 | 1H
P7 | 12.00 usec
PL7 | -1.00 dB
SFO7 | 400.151993 MHz

===== CHANNEL f8 =====
NUC8 | 1H
P8 | 12.00 usec
PL8 | -1.00 dB
SFO8 | 400.151993 MHz

===== CHANNEL f9 =====
NUC9 | 1H
P9 | 12.00 usec
PL9 | -1.00 dB
SFO9 | 400.151993 MHz

===== CHANNEL f10 =====
NUC10 | 1H
P10 | 12.00 usec
PL10 | -1.00 dB
SFO10 | 400.151993 MHz

===== CHANNEL f11 =====
NUC11 | 1H
P11 | 12.00 usec
PL11 | -1.00 dB
SFO11 | 400.151993 MHz

===== CHANNEL f12 =====
NUC12 | 1H
P12 | 12.00 usec
PL12 | -1.00 dB
SFO12 | 400.151993 MHz

===== CHANNEL f13 =====
NUC13 | 1H
P13 | 12.00 usec
PL13 | -1.00 dB
SFO13 | 400.151993 MHz

===== CHANNEL f14 =====
NUC14 | 1H
P14 | 12.00 usec
PL14 | -1.00 dB
SFO14 | 400.151993 MHz

===== CHANNEL f15 =====
NUC15 | 1H
P15 | 12.00 usec
PL15 | -1.00 dB
SFO15 | 400.151993 MHz

===== CHANNEL f16 =====
NUC16 | 1H
P16 | 12.00 usec
PL16 | -1.00 dB
SFO16 | 400.151993 MHz

===== CHANNEL f17 =====
NUC17 | 1H
P17 | 12.00 usec
PL17 | -1.00 dB
SFO17 | 400.151993 MHz

===== CHANNEL f18 =====
NUC18 | 1H
P18 | 12.00 usec
PL18 | -1.00 dB
SFO18 | 400.151993 MHz

===== CHANNEL f19 =====
NUC19 | 1H
P19 | 12.00 usec
PL19 | -1.00 dB
SFO19 | 400.151993 MHz

===== CHANNEL f20 =====
NUC20 | 1H
P20 | 12.00 usec
PL20 | -1.00 dB
SFO20 | 400.151993 MHz

===== CHANNEL f21 =====
NUC21 | 1H
P21 | 12.00 usec
PL21 | -1.00 dB
SFO21 | 400.151993 MHz

===== CHANNEL f22 =====
NUC22 | 1H
P22 | 12.00 usec
PL22 | -1.00 dB
SFO22 | 400.151993 MHz

===== CHANNEL f23 =====
NUC23 | 1H
P23 | 12.00 usec
PL23 | -1.00 dB
SFO23 | 400.151993 MHz

===== CHANNEL f24 =====
NUC24 | 1H
P24 | 12.00 usec
PL24 | -1.00 dB
SFO24 | 400.151993 MHz

===== CHANNEL f25 =====
NUC25 | 1H
P25 | 12.00 usec
PL25 | -1.00 dB
SFO25 | 400.151993 MHz

===== CHANNEL f26 =====
NUC26 | 1H
P26 | 12.00 usec
PL26 | -1.00 dB
SFO26 | 400.151993 MHz

===== CHANNEL f27 =====
NUC27 | 1H
P27 | 12.00 usec
PL27 | -1.00 dB
SFO27 | 400.151993 MHz

===== CHANNEL f28 =====
NUC28 | 1H
P28 | 12.00 usec
PL28 | -1.00 dB
SFO28 | 400.151993 MHz

===== CHANNEL f29 =====
NUC29 | 1H
P29 | 12.00 usec
PL29 | -1.00 dB
SFO29 | 400.151993 MHz

===== CHANNEL f30 =====
NUC30 | 1H
P30 | 12.00 usec
PL30 | -1.00 dB
SFO30 | 400.151993 MHz

===== CHANNEL f31 =====
NUC31 | 1H
P31 | 12.00 usec
PL31 | -1.00 dB
SFO31 | 400.151993 MHz

===== CHANNEL f32 =====
NUC32 | 1H
P32 | 12.00 usec
PL32 | -1.00 dB
SFO32 | 400.151993 MHz

===== CHANNEL f33 =====
NUC33 | 1H
P33 | 12.00 usec
PL33 | -1.00 dB
SFO33 | 400.151993 MHz

===== CHANNEL f34 =====
NUC34 | 1H
P34 | 12.00 usec
PL34 | -1.00 dB
SFO34 | 400.151993 MHz

===== CHANNEL f35 =====
NUC35 | 1H
P35 | 12.00 usec
PL35 | -1.00 dB
SFO35 | 400.151993 MHz

===== CHANNEL f36 =====
NUC36 | 1H
P36 | 12.00 usec
PL36 | -1.00 dB
SFO36 | 400.151993 MHz

===== CHANNEL f37 =====
NUC37 | 1H
P37 | 12.00 usec
PL37 | -1.00 dB
SFO37 | 400.151993 MHz

===== CHANNEL f38 =====
NUC38 | 1H
P38 | 12.00 usec
PL38 | -1.00 dB
SFO38 | 400.151993 MHz

===== CHANNEL f39 =====
NUC39 | 1H
P39 | 12.00 usec
PL39 | -1.00 dB
SFO39 | 400.151993 MHz

===== CHANNEL f40 =====
NUC40 | 1H
P40 | 12.00 usec
PL40 | -1.00 dB
SFO40 | 400.151993 MHz

===== CHANNEL f41 =====
NUC41 | 1H
P41 | 12.00 usec
PL41 | -1.00 dB
SFO41 | 400.151993 MHz

===== CHANNEL f42 =====
NUC42 | 1H
P42 | 12.00 usec
PL42 | -1.00 dB
SFO42 | 400.151993 MHz

===== CHANNEL f43 =====
NUC43 | 1H
P43 | 12.00 usec
PL43 | -1.00 dB
SFO43 | 400.151993 MHz

===== CHANNEL f44 =====
NUC44 | 1H
P44 | 12.00 usec
PL44 | -1.00 dB
SFO44 | 400.151993 MHz

===== CHANNEL f45 =====
NUC45 | 1H
P45 | 12.00 usec
PL45 | -1.00 dB
SFO45 | 400.151993 MHz

===== CHANNEL f46 =====
NUC46 | 1H
P46 | 12.00 usec
PL46 | -1.00 dB
SFO46 | 400.151993 MHz

===== CHANNEL f47 =====
NUC47 | 1H
P47 | 12.00 usec
PL47 | -1.00 dB
SFO47 | 400.151993 MHz

===== CHANNEL f48 =====
NUC48 | 1H
P48 | 12.00 usec
PL48 | -1.00 dB
SFO48 | 400.151993 MHz

===== CHANNEL f49 =====
NUC49 | 1H
P49 | 12.00 usec
PL49 | -1.00 dB
SFO49 | 400.151993 MHz

===== CHANNEL f50 =====
NUC50 | 1H
P50 | 12.00 usec
PL50 | -1.00 dB
SFO50 | 400.151993 MHz

===== CHANNEL f51 =====
NUC51 | 1H
P51 | 12.00 usec
PL51 | -1.00 dB
SFO51 | 400.151993 MHz

===== CHANNEL f52 =====
NUC52 | 1H
P52 | 12.00 usec
PL52 | -1.00 dB
SFO52 | 400.151993 MHz

===== CHANNEL f53 =====
NUC53 | 1H
P53 | 12.00 usec
PL53 | -1.00 dB
SFO53 | 400.151993 MHz

===== CHANNEL f54 =====
NUC54 | 1H
P54 | 12.00 usec
PL54 | -1.00 dB
SFO54 | 400.151993 MHz

===== CHANNEL f55 =====
NUC55 | 1H
P55 | 12.00 usec
PL55 | -1.00 dB
SFO55 | 400.151993 MHz

===== CHANNEL f56 =====
NUC56 | 1H
P56 | 12.00 usec
PL56 | -1.00 dB
SFO56 | 400.151993 MHz

===== CHANNEL f57 =====
NUC57 | 1H
P57 | 12.00 usec
PL57 | -1.00 dB
SFO57 | 400.151993 MHz

===== CHANNEL f58 =====
NUC58 | 1H
P58 | 12.00 usec
PL58 | -1.00 dB
SFO58 | 400.151993 MHz

===== CHANNEL f59 =====
NUC59 | 1H
P59 | 12.00 usec
PL59 | -1.00 dB
SFO59 | 400.151993 MHz

===== CHANNEL f60 =====
NUC60 | 1H
P60 | 12.00 usec
PL60 | -1.00 dB
SFO60 | 400.151993 MHz

===== CHANNEL f61 =====
NUC61 | 1H
P61 | 12.00 usec
PL61 | -1.00 dB
SFO61 | 400.151993 MHz

===== CHANNEL f62 =====
NUC62 | 1H
P62 | 12.00 usec
PL62 | -1.00 dB
SFO62 | 400.151993 MHz

===== CHANNEL f63 =====
NUC63 | 1H
P63 | 12.00 usec
PL63 | -1.00 dB
SFO63 | 400.151993 MHz

===== CHANNEL f64 =====
NUC64 | 1H
P64 | 12.00 usec
PL64 | -1.00 dB
SFO64 | 400.151993 MHz

===== CHANNEL f65 =====
NUC65 | 1H
P65 | 12.00 usec
PL65 | -1.00 dB
SFO65 | 400.151993 MHz

===== CHANNEL f66 =====
NUC66 | 1H
P66 | 12.00 usec
PL66 | -1.00 dB
SFO66 | 400.151993 MHz

===== CHANNEL f67 =====
NUC67 | 1H
P67 | 12.00 usec
PL67 | -1.00 dB
SFO67 | 400.151993 MHz

===== CHANNEL f68 =====
NUC68 | 1H
P68 | 12.00 usec
PL68 | -1.00 dB
SFO68 | 400.151993 MHz

===== CHANNEL f69 =====
NUC69 | 1H
P69 | 12.00 usec
PL69 | -1.00 dB
SFO69 | 400.151993 MHz

===== CHANNEL f70 =====
NUC70 | 1H
P70 | 12.00 usec
PL70 | -1.00 dB
SFO70 | 400.151993 MHz

===== CHANNEL f71 =====
NUC71 | 1H
P71 | 12.00 usec
PL71 | -1.00 dB
SFO71 | 400.151993 MHz

===== CHANNEL f72 =====
NUC72 | 1H
P72 | 12.00 usec
PL72 | -1.00 dB
SFO72 | 400.151993 MHz

===== CHANNEL f73 =====
NUC73 | 1H
P73 | 12.00 usec
PL73 | -1.00 dB
SFO73 | 400.151993 MHz

===== CHANNEL f74 =====
NUC74 | 1H
P74 | 12.00 usec
PL74 | -1.00 dB
SFO74 | 400.151993 MHz

===== CHANNEL f75 =====
NUC75 | 1H
P75 | 12.00 usec
PL75 | -1.00 dB
SFO75 | 400.151993 MHz

===== CHANNEL f76 =====
NUC76 | 1H
P76 | 12.00 usec
PL76 | -1.00 dB
SFO76 | 400.151993 MHz

===== CHANNEL f77 =====
NUC77 | 1H
P77 | 12.00 usec
PL77 | -1.00 dB
SFO77 | 400.151993 MHz

===== CHANNEL f78 =====
NUC78 | 1H
P78 | 12.00 usec
PL78 | -1.00 dB
SFO78 | 400.151993 MHz

===== CHANNEL f79 =====
NUC79 | 1H
P79 | 12.00 usec
PL79 | -1.00 dB
SFO79 | 400.151993 MHz

===== CHANNEL f80 =====
NUC80 | 1H
P80 | 12.00 usec
PL80 | -1.00 dB
SFO80 | 400.151993 MHz

===== CHANNEL f81 =====
NUC81 | 1H
P81 | 12.00 usec
PL81 | -1.00 dB
SFO81 | 400.151993 MHz

===== CHANNEL f82 =====
NUC82 | 1H
P82 | 12.00 usec
PL82 | -1.00 dB
SFO82 | 400.151993 MHz

===== CHANNEL f83 =====
NUC83 | 1H
P83 | 12.00 usec
PL83 | -1.00 dB
SFO83 | 400.151993 MHz

===== CHANNEL f84 =====
NUC84 | 1H
P84 | 12.00 usec
PL84 | -1.00 dB
SFO84 | 400.151993 MHz

===== CHANNEL f85 =====
NUC85 | 1H
P85 | 12.00 usec
PL85 | -1.00 dB
SFO85 | 400.151993 MHz

===== CHANNEL f86 =====
NUC86 | 1H
P86 | 12.00 usec
PL86 | -1.00 dB
SFO86 | 400.151993 MHz

===== CHANNEL f87 =====
NUC87 | 1H
P87 | 12.00 usec
PL87 | -1.00 dB
SFO87 | 400.151993 MHz

===== CHANNEL f88 =====
NUC88 | 1H
P88 | 12.00 usec
PL88 | -1.00 dB
SFO88 | 400.151993 MHz

===== CHANNEL f89 =====
NUC89 | 1H
P89 | 12.00 usec
PL89 | -1.00 dB
SFO89 | 400.151993 MHz

===== CHANNEL f90 =====
NUC90 | 1H
P90 | 12.00 usec
PL90 | -1.00 dB
SFO90 | 400.151993 MHz

===== CHANNEL f91 =====
NUC91 | 1H
P91 | 12.00 usec
PL91 | -1.00 dB
SFO91 | 400.151993 MHz

===== CHANNEL f92 =====
NUC92 | 1H
P92 | 12.00 usec
PL92 | -1.00 dB
SFO92 | 400.151993 MHz

===== CHANNEL f93 =====
NUC93 | 1H
P93 | 12.00 usec
PL93 | -1.00 dB
SFO93 | 400.151993 MHz

===== CHANNEL f94 =====
NUC94 | 1H
P94 | 12.00 usec
PL94 | -1.00 dB
SFO94 | 400.151993 MHz

===== CHANNEL f95 =====
NUC95 | 1H
P95 | 12.00 usec
PL95 | -1.00 dB
SFO95 | 400.151993 MHz

===== CHANNEL f96 =====
NUC96 | 1H
P96 | 12.00 usec
PL96 | -1.00 dB
SFO96 | 400.151993 MHz

===== CHANNEL f97 =====
NUC97 | 1H
P97 | 12.00 usec
PL97 | -1.00 dB
SFO97 | 400.151993 MHz

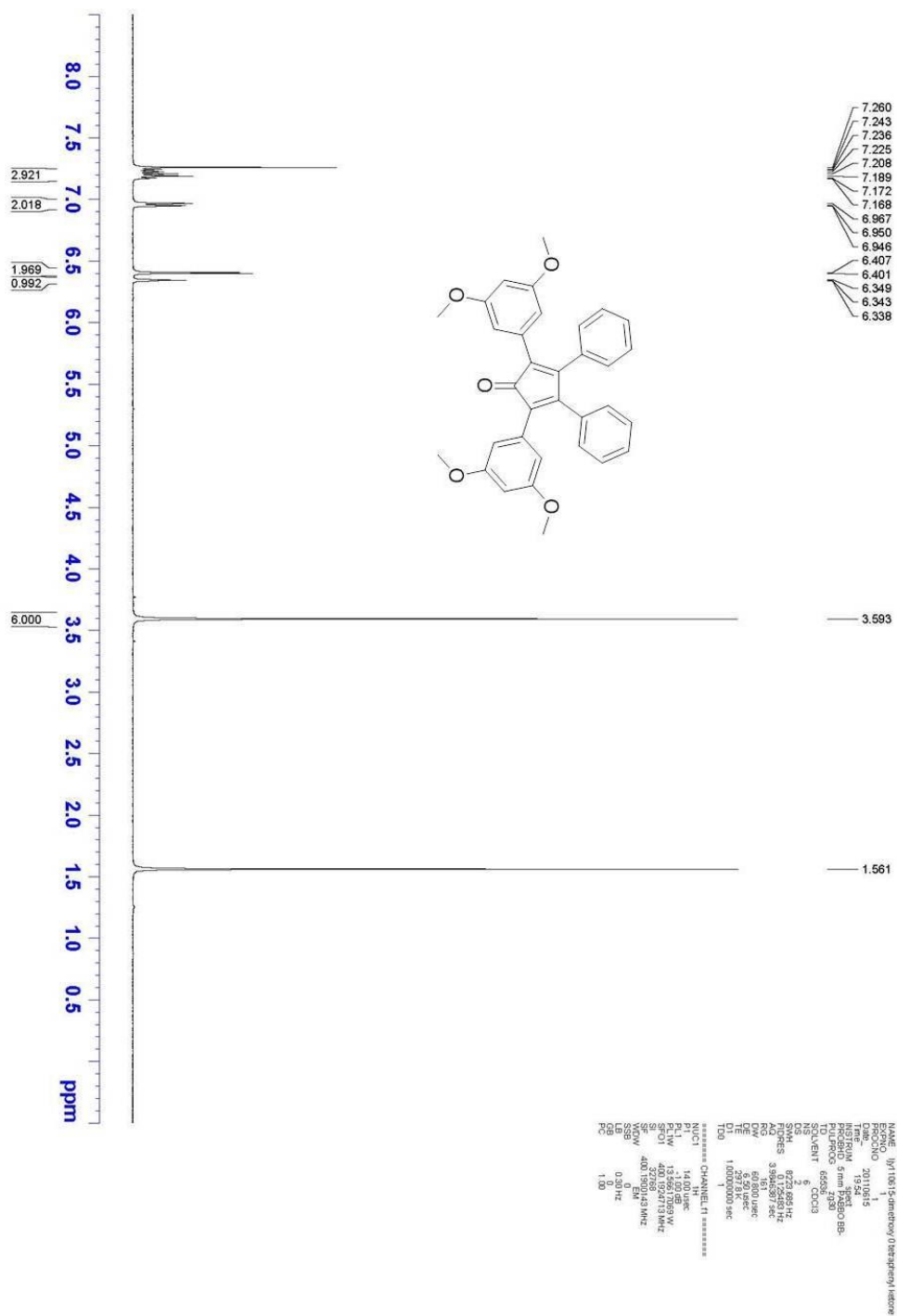
===== CHANNEL f98 =====
NUC98 | 1H
P98 | 12.00 usec
PL98 | -1.00 dB
SFO98 | 400.151993 MHz

===== CHANNEL f99 =====
NUC99 | 1H
P99 | 12.00 usec
PL99 | -1.00 dB
SFO99 | 400.151993 MHz

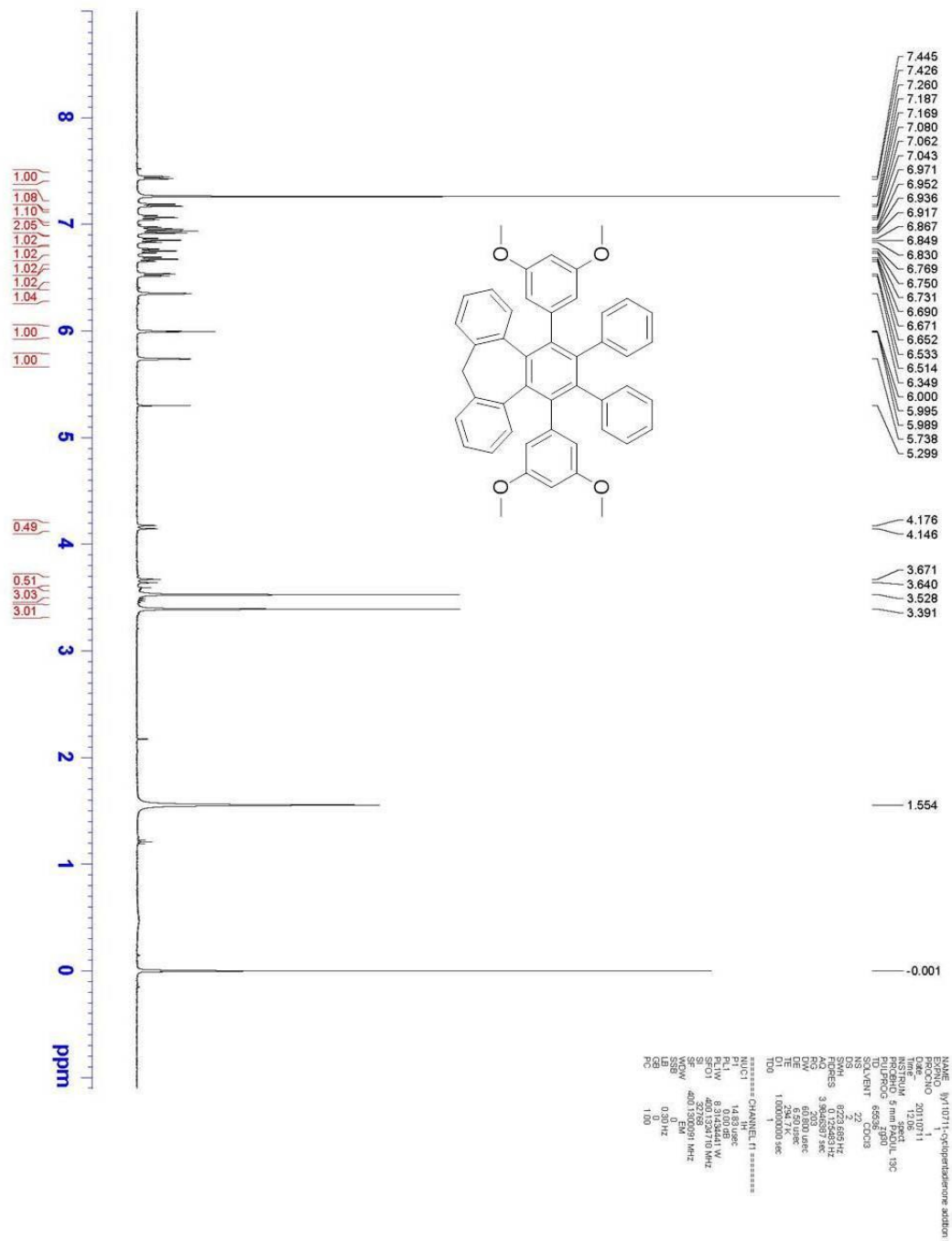
===== CHANNEL f100 =====
NUC100 | 1H
P100 | 12.00 usec
PL100 | -1.00 dB
SFO100 | 400.151993 MHz

```

¹³C NMR spectrum of 12

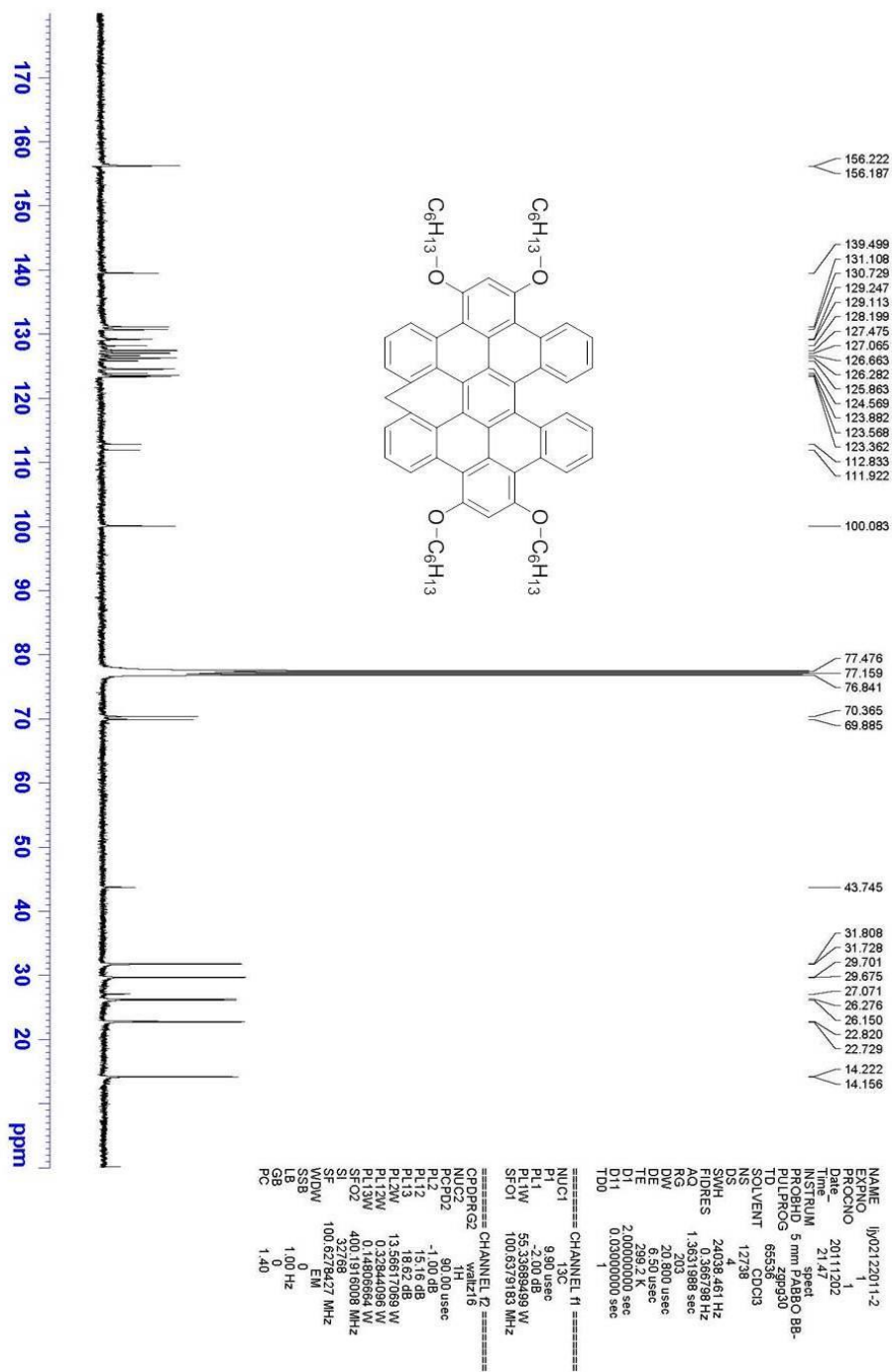


¹H NMR spectrum of **3**

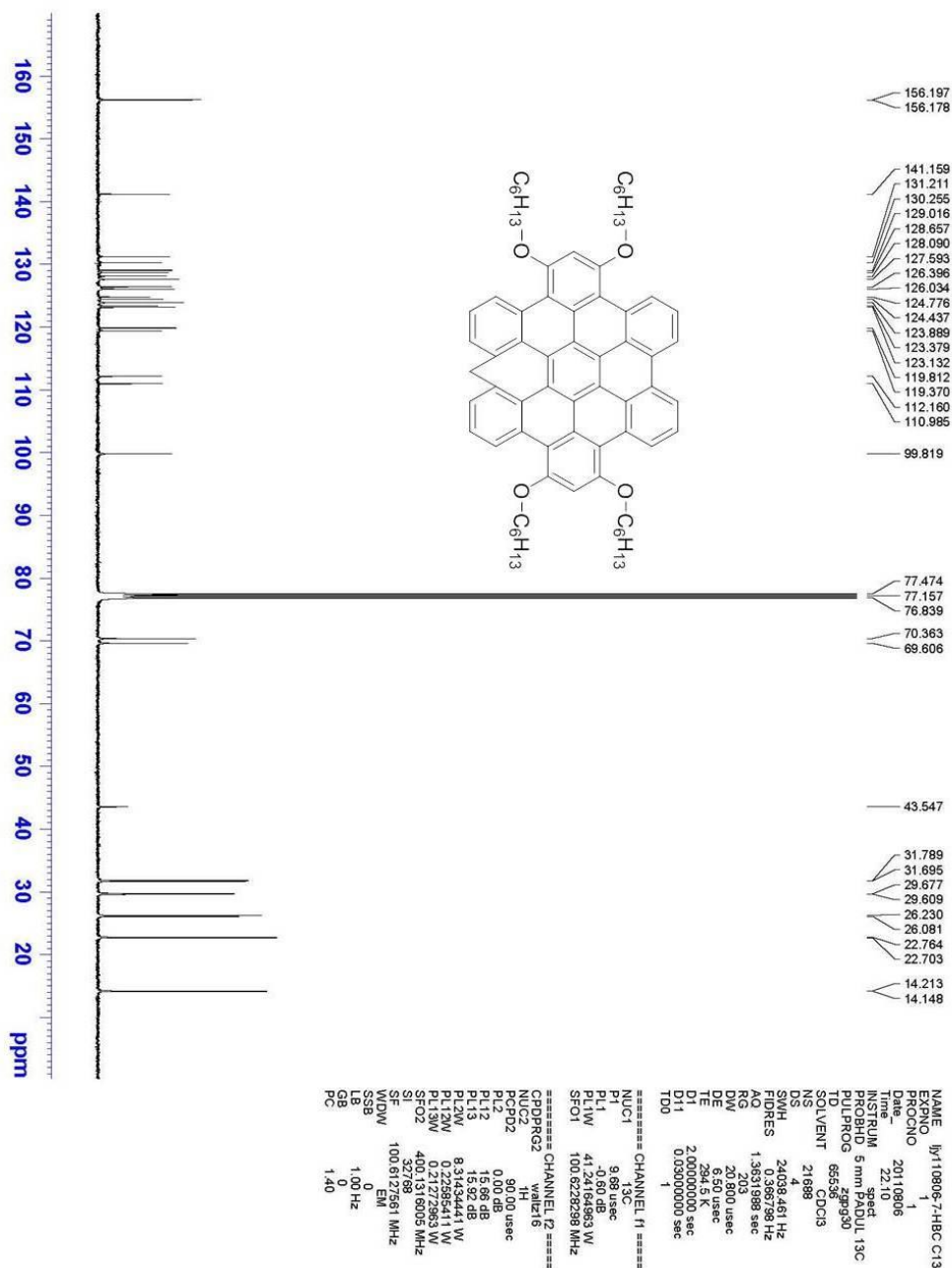


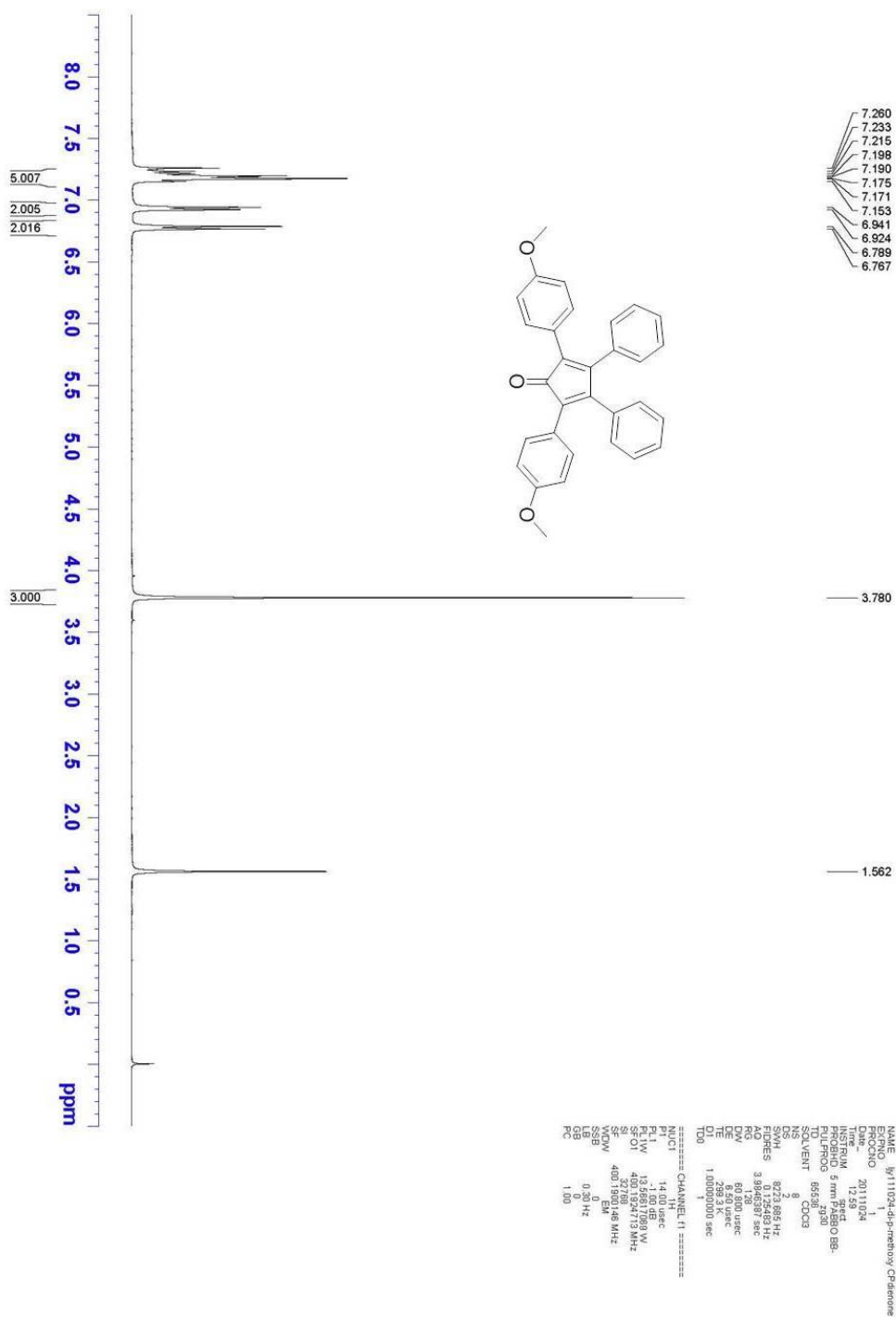
¹H NMR spectrum of **13**



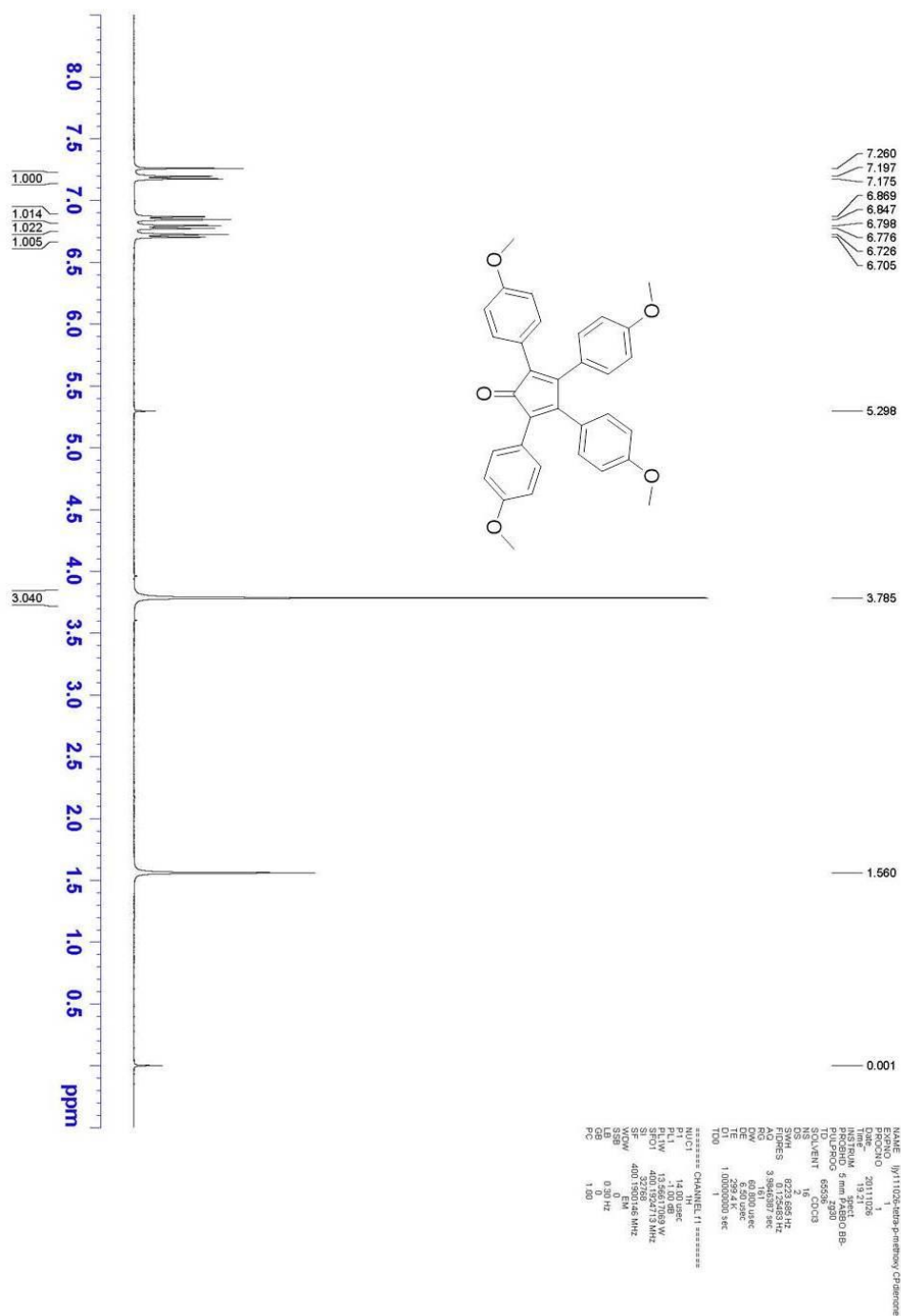


¹³C NMR spectrum of **8**



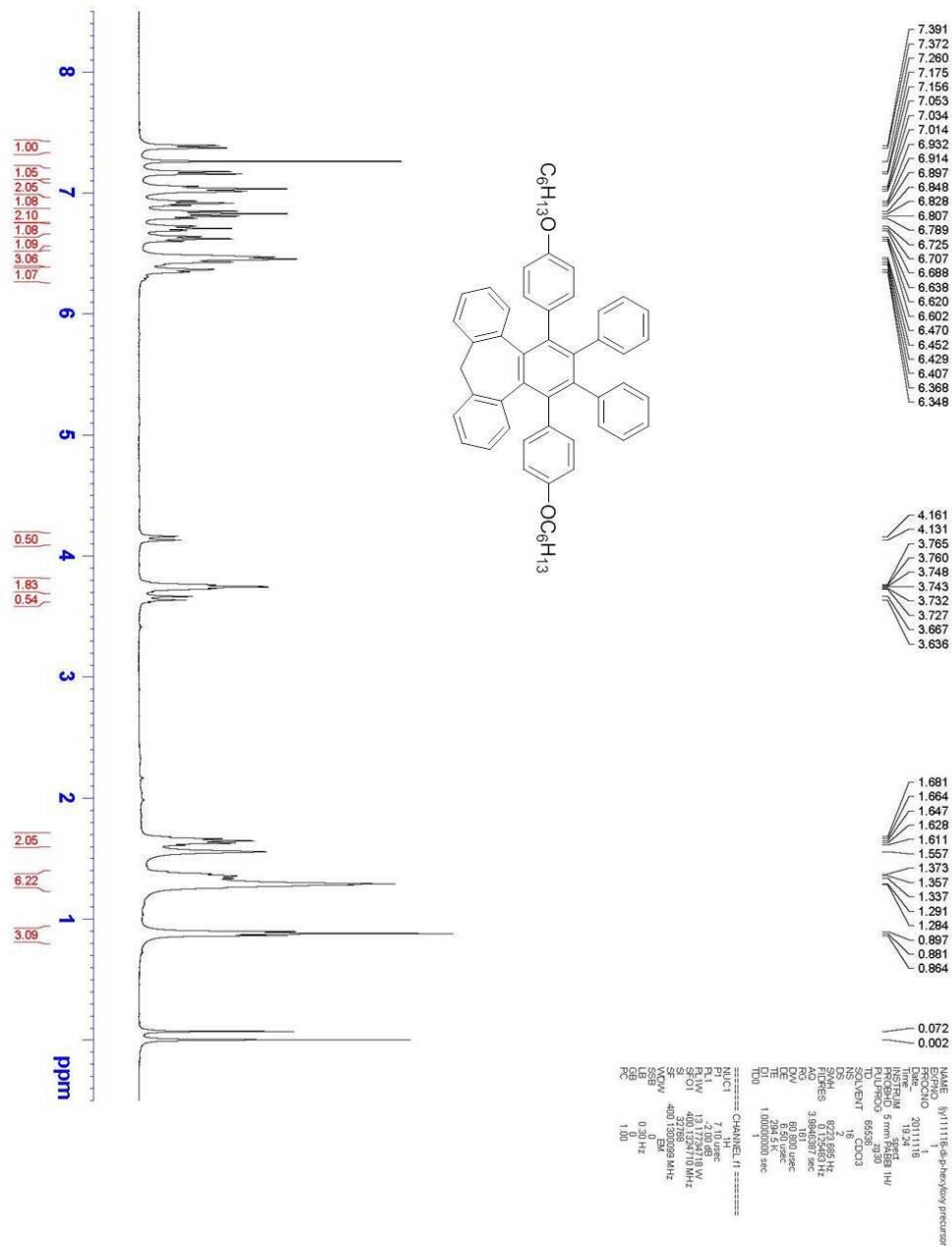


¹H NMR spectrum of 14



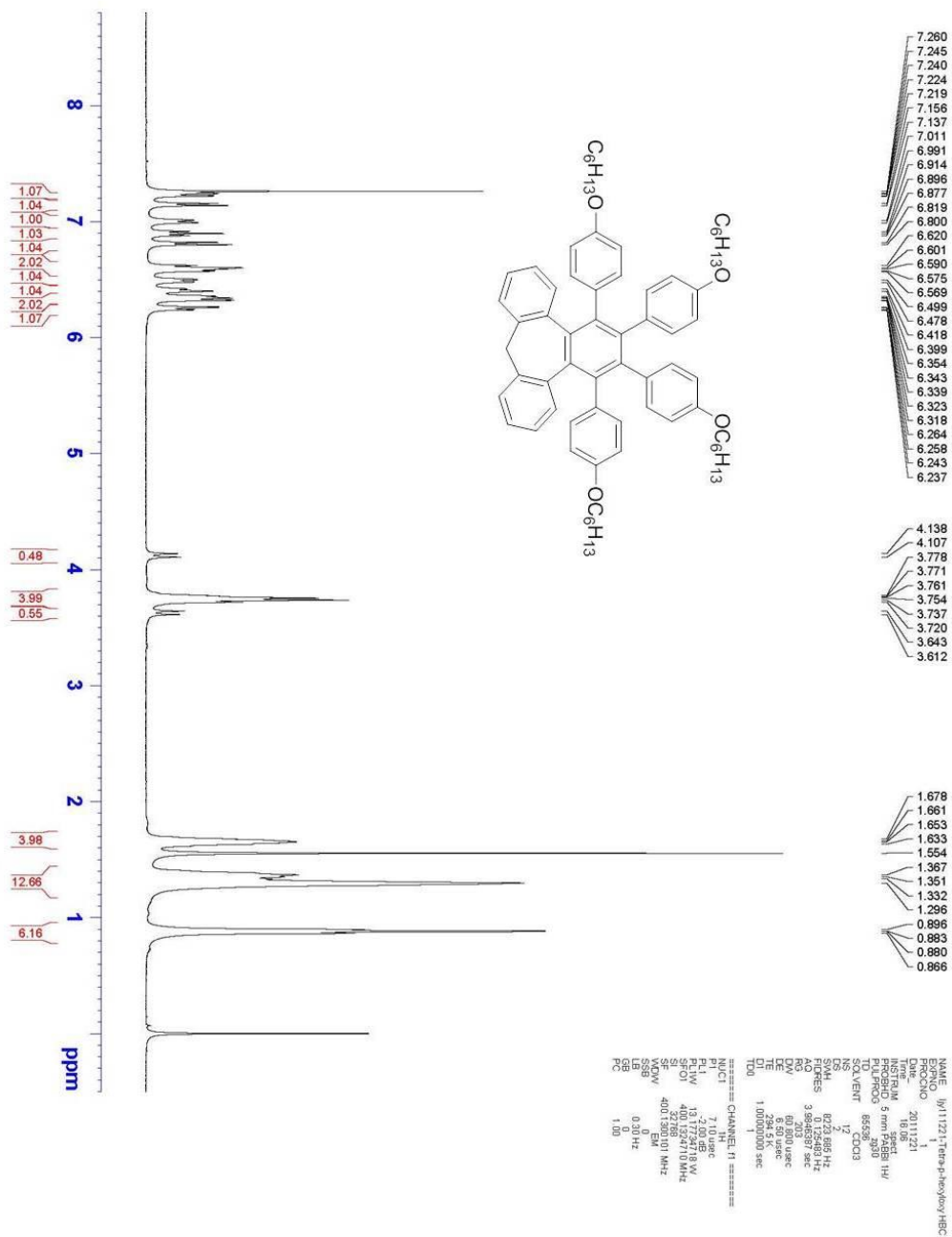
^1H NMR spectrum of **15**

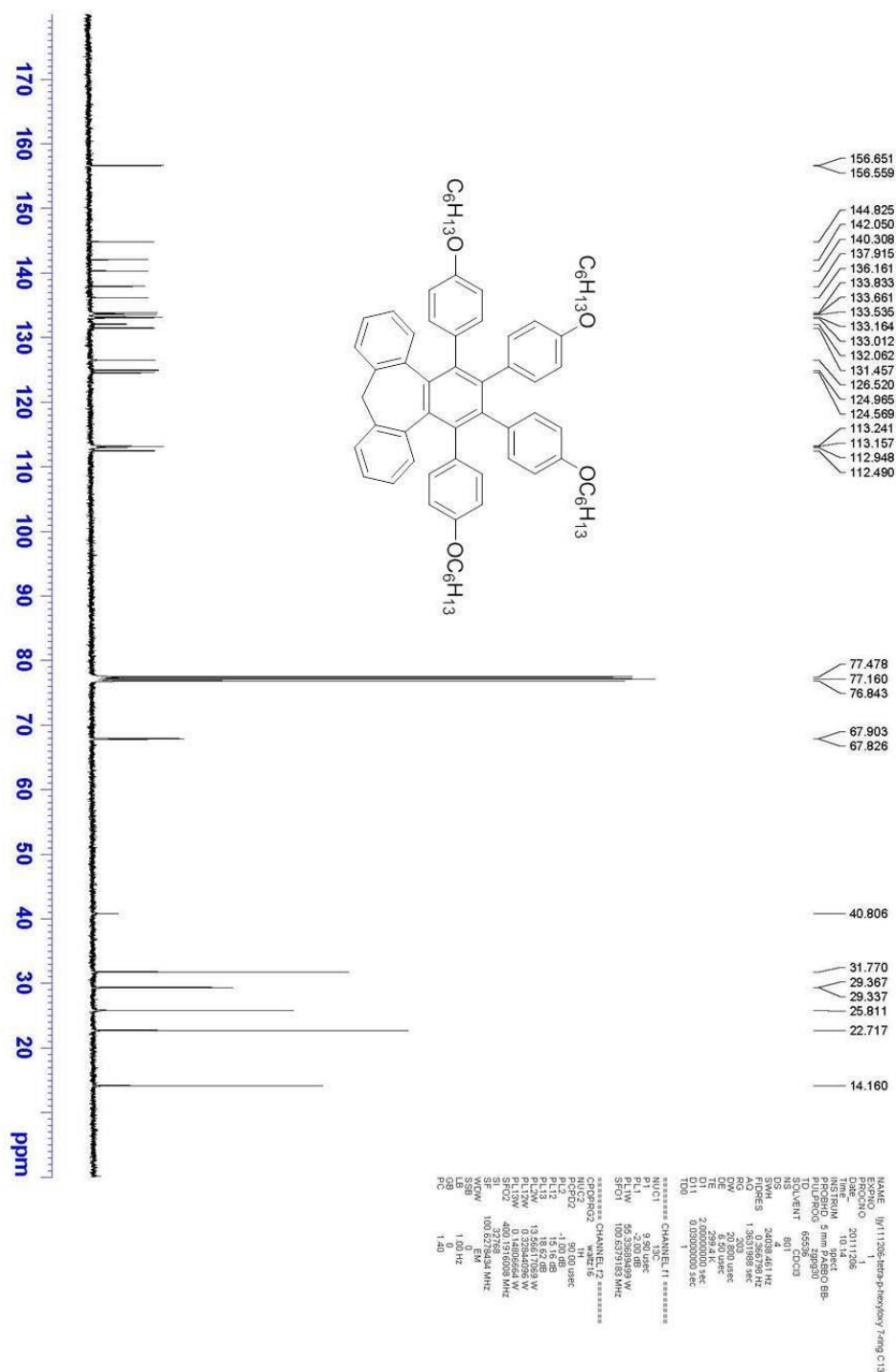


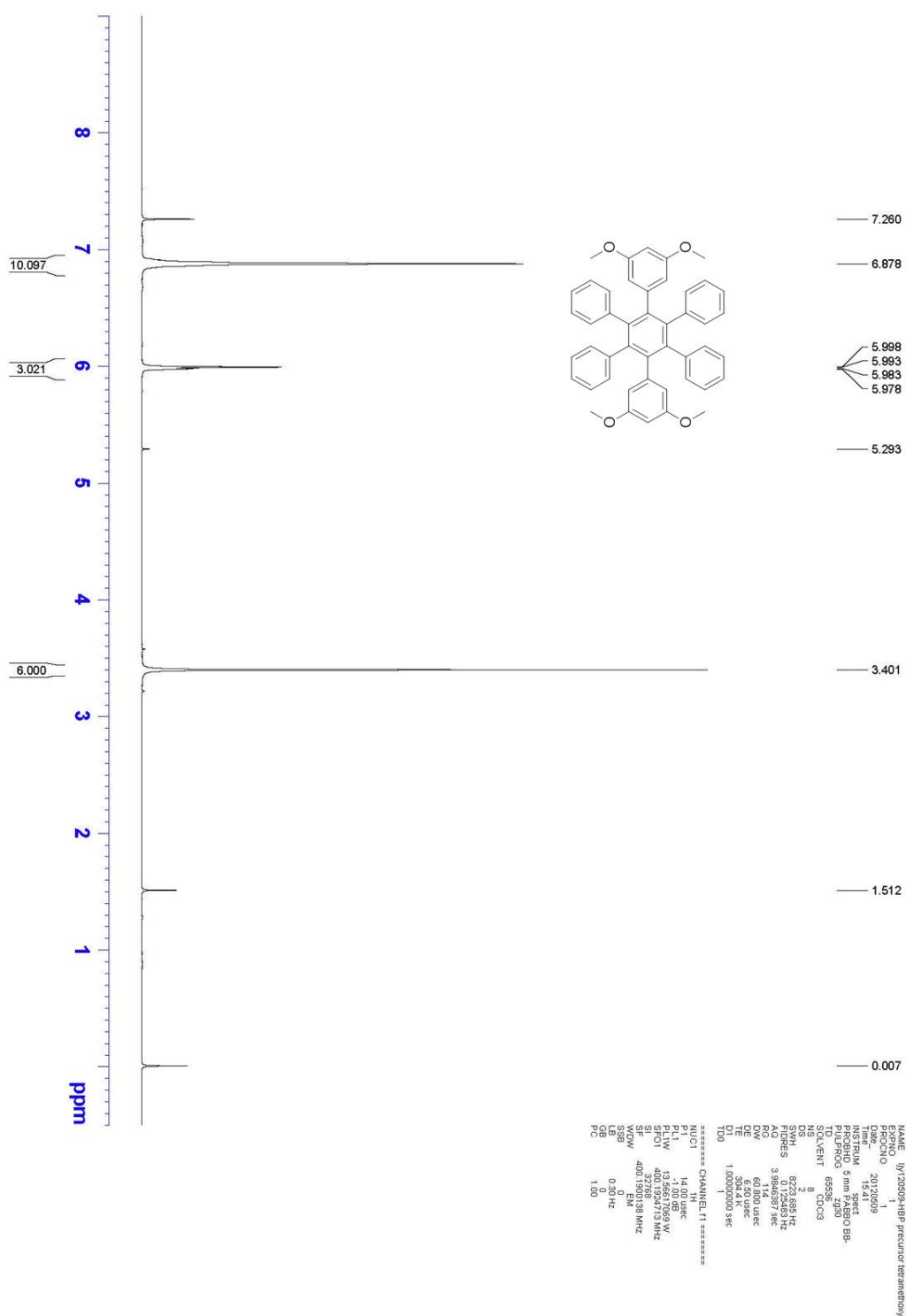


¹H NMR spectrum of **6**

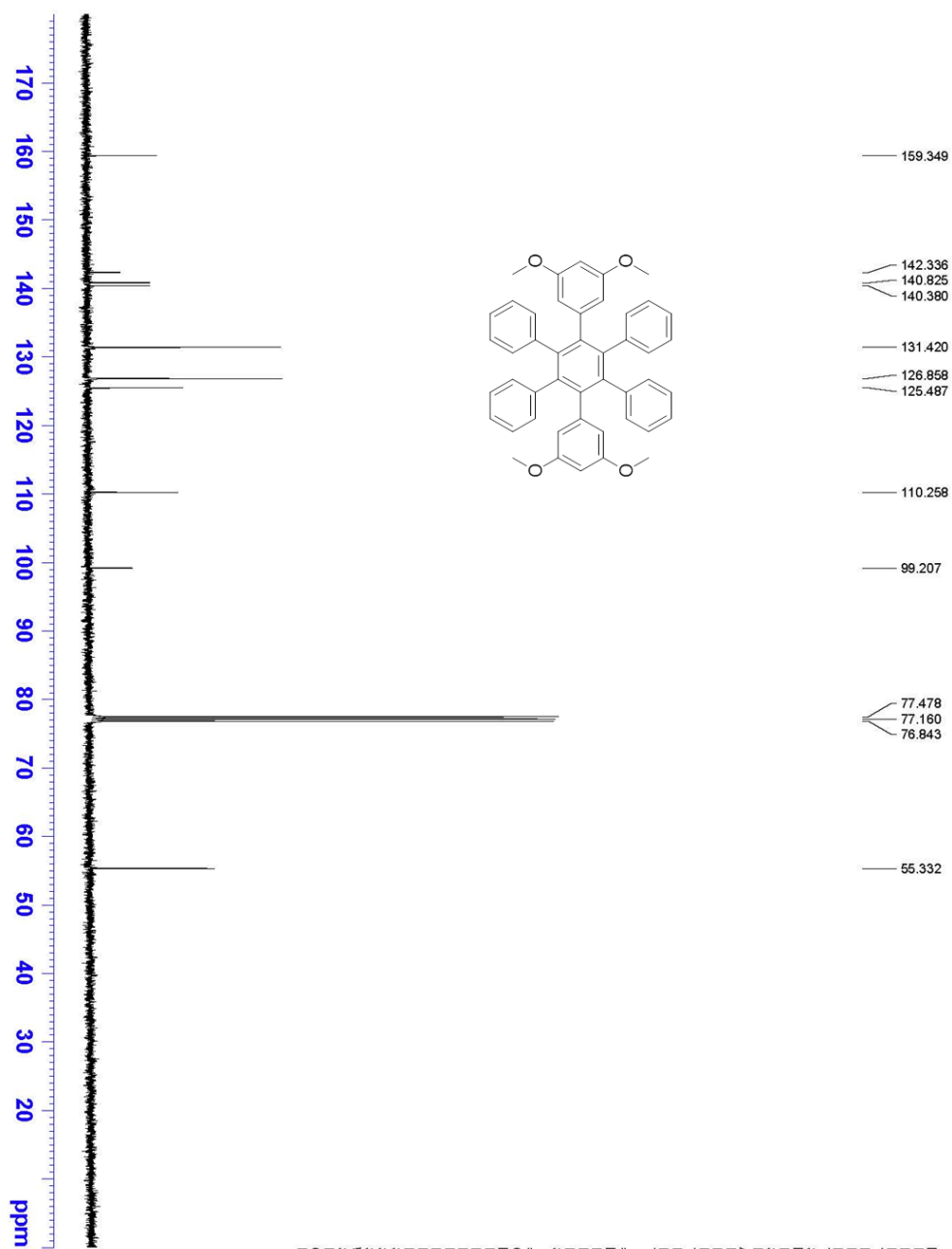
^{13}C NMR spectrum of **6**







¹H NMR spectrum of **10a**



```

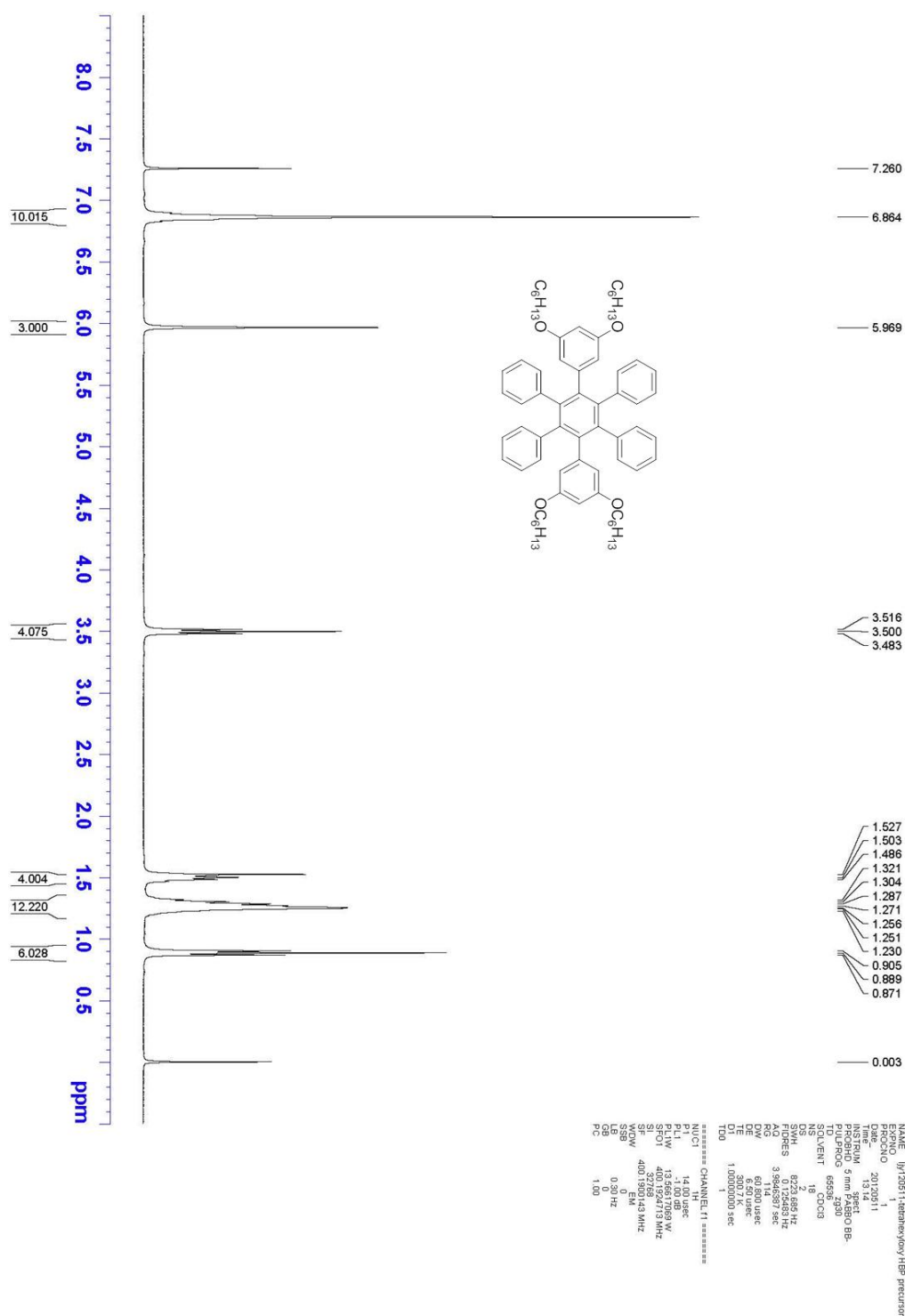
NAME |j120509-HBP precursor tetramethoxy
EXPNO 1
PROCNO 1
Date_ 20120509
Time 15.45
INSTRUM spect
PROBHD 5 mm PABBO BB-
PULPROG zgpg30
TD 65536
SOLVENT CDCl3
NS 118
DS 4
SWH 24038.461 Hz
FIDRES 0.366798 Hz
AQ 1.3631988 sec
RG 18
AQ 20.680 usec
DE 6.50 usec
TE 303.5 K
D1 2.00000000 sec
D11 0.03000000 sec
TD0 1

===== CHANNEL f1 =====
NUC1 13C
P1 9.90 usec
PL1 -2.00 dB
PL1W 55.3369499 W
SFO1 100.6379183 MHz

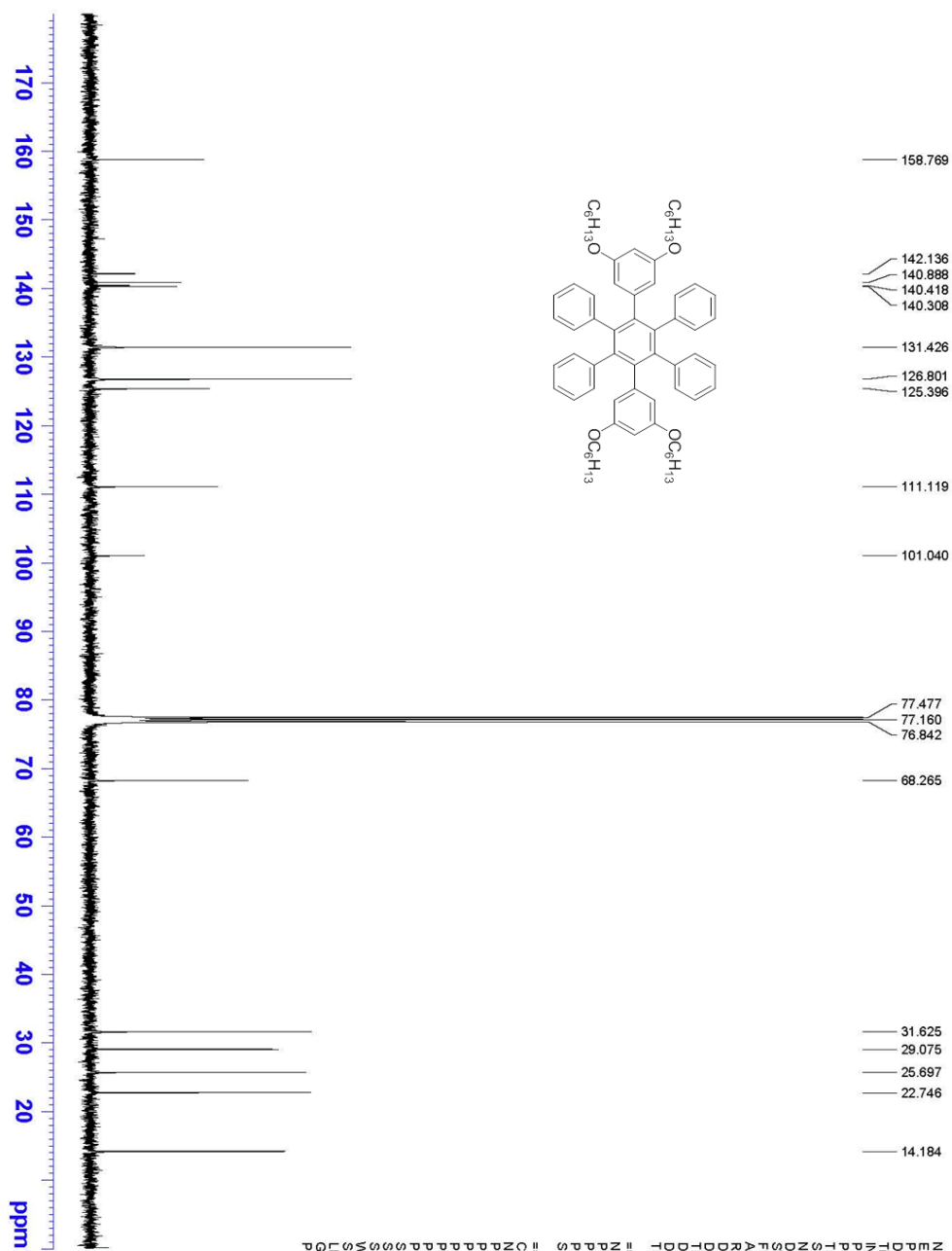
===== CHANNEL f2 =====
CPDPRG2 waltz16
NUC2 1H
PCPD2 1.00 usec
PL2 -1.00 dB
PL12 15.16 dB
PL13 18.62 dB
PL12W 13.56817069 W
PL12W 0.32844086 W
PL13W 1.01389064 W
SFO2 400.1516008 MHz
SI 32768
SF 100.6278412 MHz
WDW EM
SSB 0
LB 1.00 Hz
GB 0
PC 1.40

```

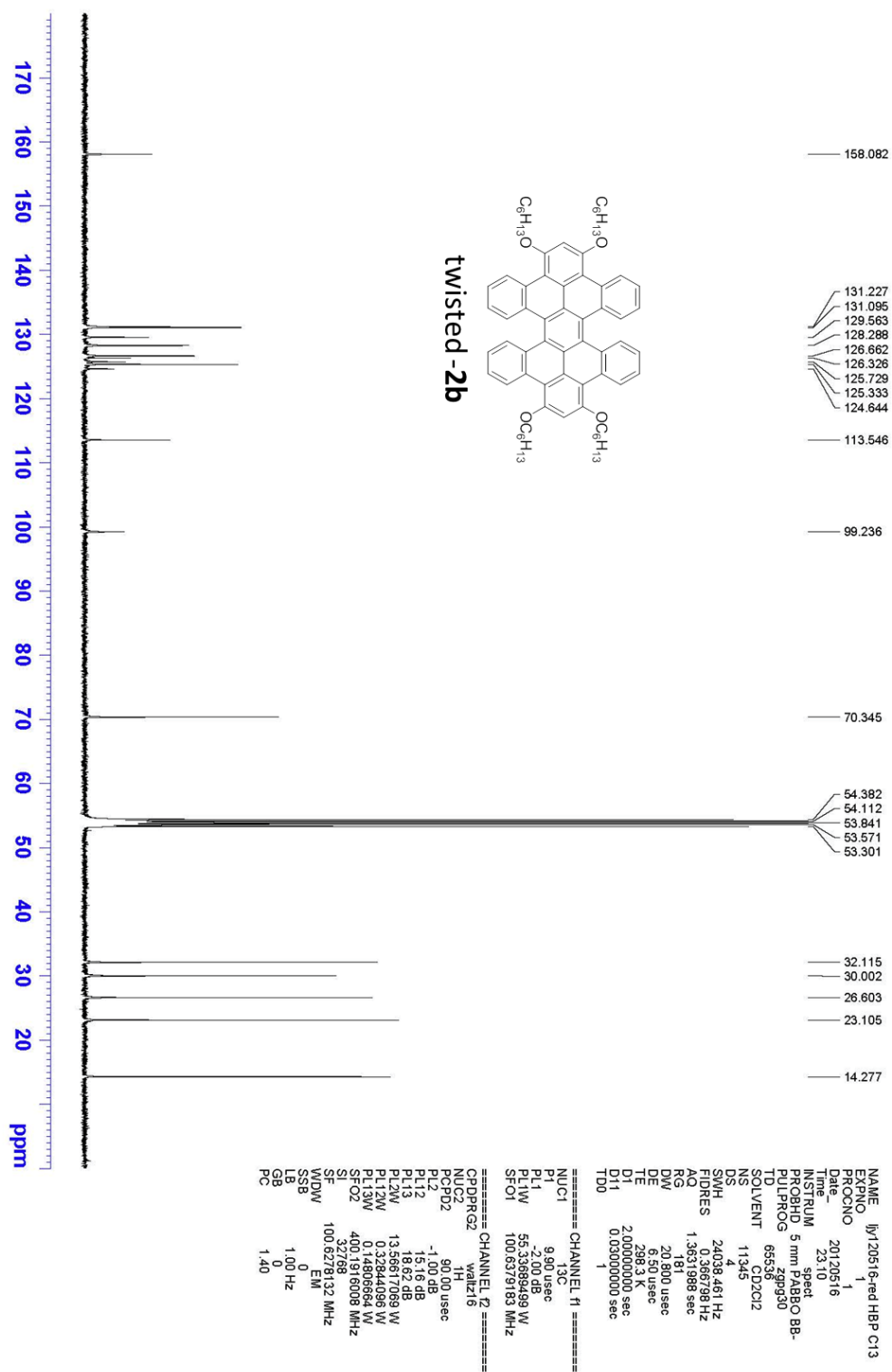
¹³C NMR spectrum of **10a**



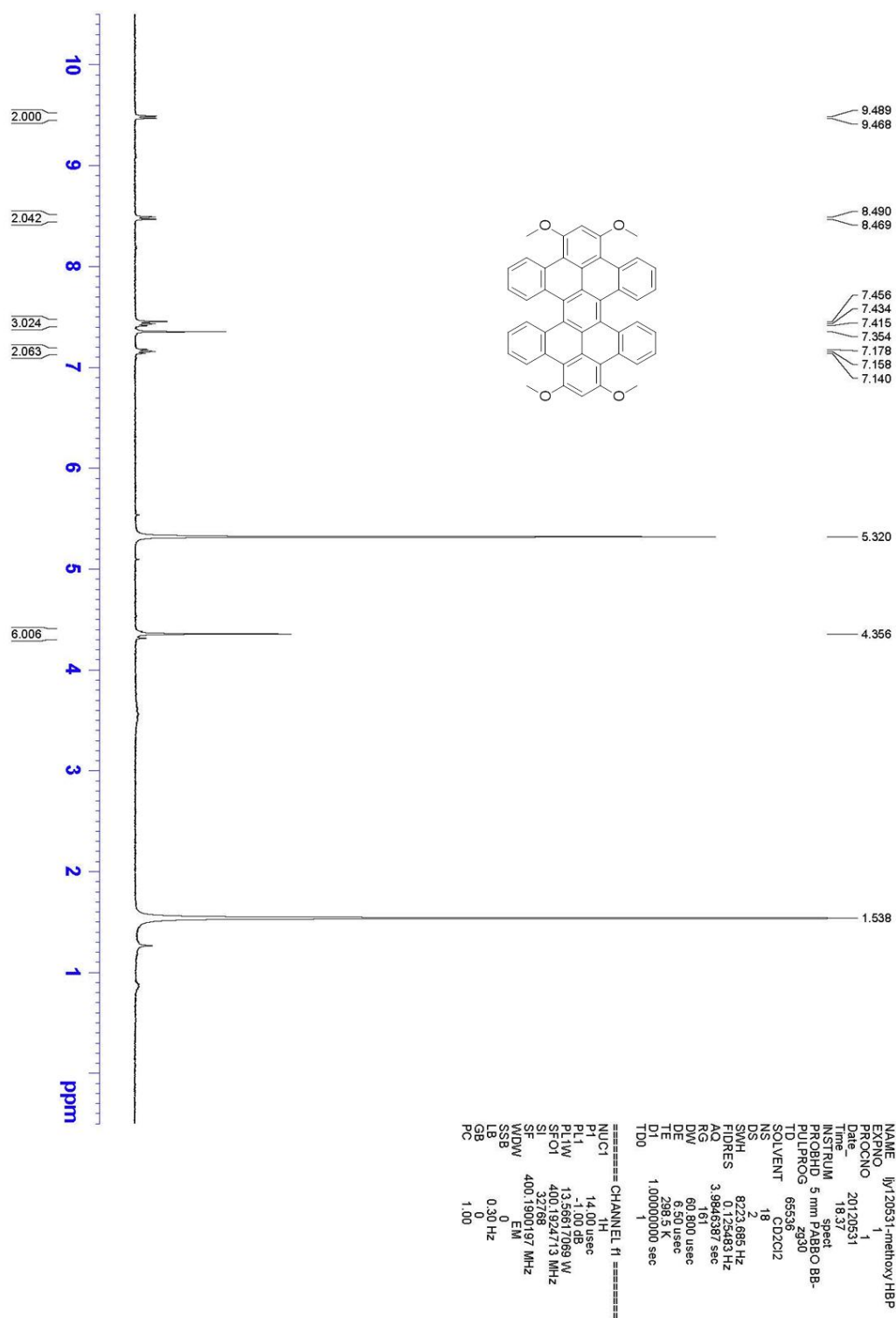
¹H NMR spectrum of **10b**



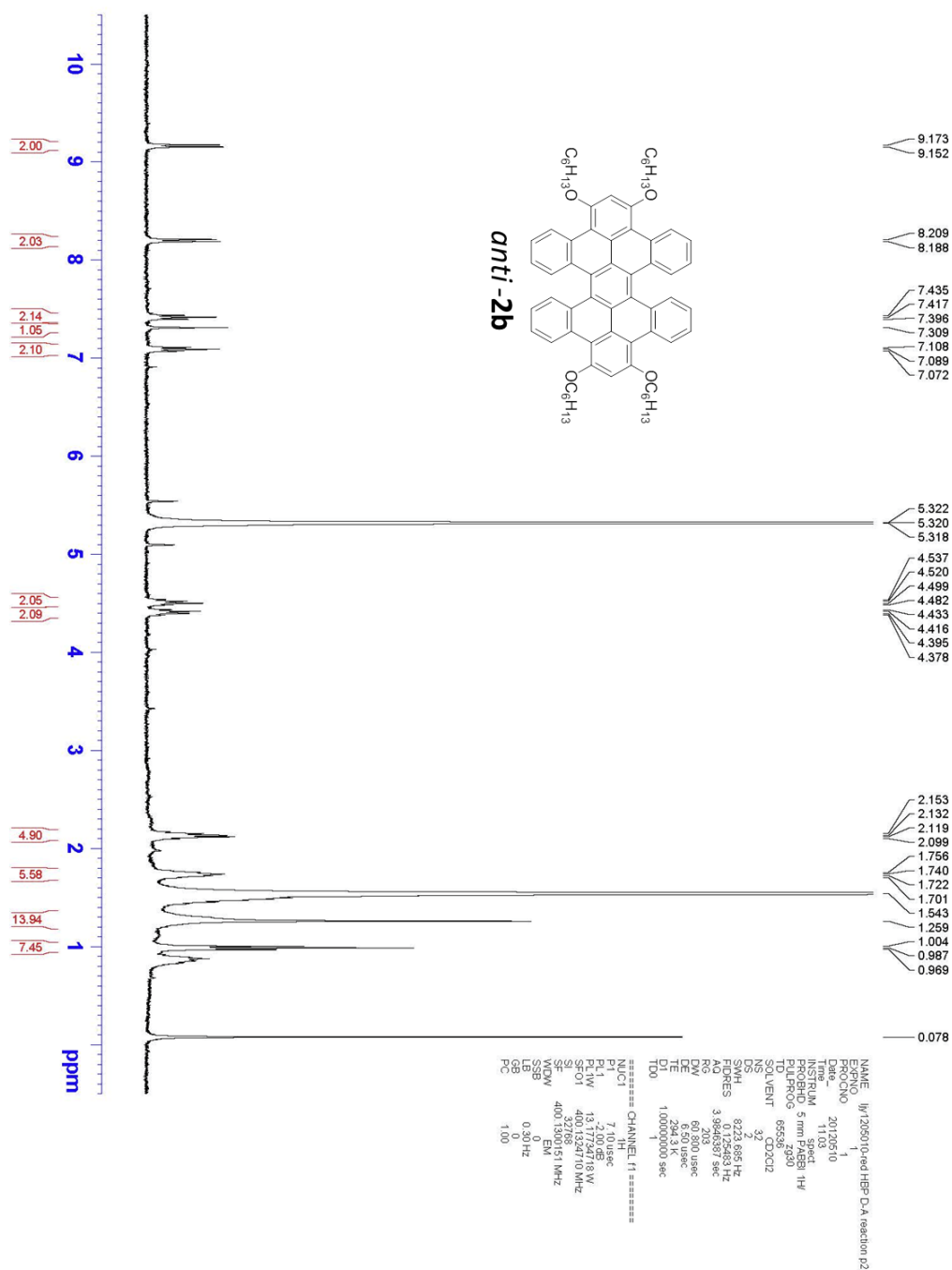
¹³C NMR spectrum of **10b**



^{13}C NMR spectrum of twisted-2b



¹H NMR spectrum of **2a**



¹H NMR spectrum of *anti-2b*

9. Calculation of Gauss Curvature (by Dr. Yi Liu, Department of Mathematics, University of California, Berkeley)

Geometry of simplicial surfaces in the 3D space ⁵

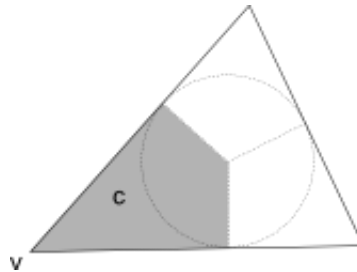
This section provides some general formulation of geometric notions for simplicial surfaces in the 3-dimensional Euclidean space E^3 . These are analogous to the smooth case where such notions are formulated using Riemannian geometry. Described below is a method of measuring how curved a simplicial surface is on average.

Let S be an embedded (or more generally, immersed) simplicial surface in E^3 . Here by *simplicial* S has been triangulated and each of the finitely many triangle pieces is flatly embedded. The vertices of the triangles are called the *vertices* of S , and they may either lie in the interior S° , or lie on the boundary ∂S , of S . For any vertex v , an *angle* θ at v is known as the corresponding angle of a triangle adjacent to v , usually denoted $\theta @ v$. With the notations above, the *total Gauss curvature* of S is defined as:

$$\iint_S K dA = \sum_{v \in S^\circ} (2\pi - \sum_{\theta @ v} \theta),$$

where the left-hand side is the usual notation. The term in the parentheses is usually called the *angle deficit* at v . It describes the local contribution of the Gauss curvature at v , and the surface is said to be positively curved, flat, or negatively curved at v depending on the sign of angle deficit.

One may describe the average Gauss curvature by dividing the total Gauss curvature by the area of the surface, but a more reasonable way is to divide by the following effective area. With the notations above, the *combinatorial corner* c at v is defined as the shaded kite region of a triangle adjacent to v (see the figure below), denoted as $c @ v$.



The *effective area* of S is defined as the sum of the area of combinatorial corners in the interior, namely:

$$A^*(S) = \sum_{v \in S^\circ} \sum_{c @ v} \text{Area}(c).$$

Then the *average Gauss curvature* of S is defined as:

$$\bar{K}(S) = \frac{\iint_S K dA}{A^*(S)}.$$

5. John M. Sullivan, *Curvatures of smooth and discrete surfaces*, Discrete Differential Geometry, 175–188, Oberwolfach Semin., 38, Birkhäuser, Basel, 2008.

For smoothly immersed surfaces in E^3 , the classical Gauss curvature describes the *intrinsic curvedness* of the surface with the induced Riemannian metric. The above definitions also feature this, and have the advantage of simpler computation. When two simplicial surfaces in E^3 have significantly different areas, the average Gauss curvature is certainly more meaningful a notion than the total Gauss curvature.

Curvature of molecules

Topologically, the carbon skeleton of a molecule can be regarded as a graph with vertices the carbon atoms and edges the bonds. Whenever there is a reasonable way to regard the graph as the skeleton of a polygonal surface, the associated curvatures can be discussed. In the current situation, the 7-circulene (a) naturally spans a polygonal surface (indeed, a topological disc) containing one heptagon and seven hexagons. The heptagon-embedded HBC (b) also spans a polygonal disc containing one heptagon and twelve hexagons. The benzylic sp^3 carbon in the seven-membered ring is not part of the π -backbone of **1**, and is thus excluded for the purpose of calculating curvature of the π -face of **1**. After exclusion of the benzylic sp^3 carbon, the π -face of **1** is regarded as a union of thirteen hexagons.

To apply the tools from the previous section, it is necessary to triangulate the faces, and realize the surface in the space by making each triangle flat and spanning its edges. The Gauss curvature of such a surface would then roughly describe the curvedness of the planar graph. Note that different triangulations may yield different numerical results, but there is a reasonable canonical choice as follows. By putting a center to each face, each hexagon is naturally triangulated into six triangles, and each heptagon into seven triangles. Then each center is placed at the space so that the total area of the surface is minimized. It turns out that the image in the space of such a triangulated surface is canonically determined, and furthermore, there is a fairly efficient algorithm computing this, using the convexity of the area functional on the positions of the centers. With this *minimal centric triangulation*, the areas and the curvatures implementing formulas from the previous section are computed from the space coordinates of carbon atoms in the crystal structure. The results are shown in the table below. (1 steradian = $(180/\pi)^2$ degree²)

Molecule	Total Area (Å ²)	Total Effective Area (Å ²)	Total Gauss Curvature		Average Gauss Curvature	
			deg ²	steradian	deg ² ·Å ⁻²	steradian·Å ⁻²
7-Circulene	43.89	27.94	-1594.4	-0.4857	-57.0	-0.01736
Heptagon-Embedded HBC (1)	68.80	43.87	-2128.1	-0.6483	-48.5	-0.01477

One might wonder how much the result depend on the choice of triangulation. Therefore the total Gauss curvature and the average Gauss curvature are also computed using triangulations that randomly place each center into the convex hull of the vertices of its corresponding face. The following table shows the statistics of 500 random samples, each obtained via a weighted barycentric triangulation, where the weight of every vertex was assigned by a random value independently evenly distributed on the interval [0,1].

Molecule	Total Gauss Curvature (deg ²)		Average Gauss Curvature (deg ² ·Å ⁻²)	
	Mean	Standard Deviation	Mean	Standard. Deviation
7-Circulene	-1605.2	23.7	-56.2	0.9
Heptagon -Embedded HBC (1)	-2133.8	61.4	-47.8	1.2

These numerical results indicate that the average Gauss curvature of these two molecules do not differ significantly, but the total Gauss curvature of the heptagon-embedded HBC is slightly greater than that of the 7-circulene in absolute value.